Estimating multi-scale irrigation amounts using multi-resolution soil moisture data: A data-driven approach using PrISM

Giovanni Paolini, Maria Jose Escorihuela, Olivier Merlin, Pierre Laluet, Joaquim Bellvert, Thierry Pellarin

Agricultural Water Management 290 (2023) 108594

Contents lists available at ScienceDirect

Agricultural Water Management

journal homepage: www.elsevier.com/locate/agwat

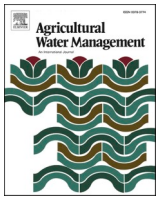

Estimating multi-scale irrigation amounts using multi-resolution soil moisture data: A data-driven approach using PrISM

Giovanni Paolini [a,*], Maria Jose Escorihuela [a], Olivier Merlin [b], Pierre Laluet [b], Joaquim Bellvert [c], Thierry Pellarin [d]

[a] isardSAT, Parc Tecnologic Barcelona Activa, Carrer de Marie Curie, 8, Barcelona 08042, Catalunya, Spain
[b] CESBIO (Centre d'Études Spatiales de la BIOsphère), University of Toulouse, CNES/CNRS/INRAE/IRD/UPS, 18 Avenue Edouard Belin, Toulouse 31401, France
[c] Efficient Use of Water in Agriculture Program, Institut de Recerca i Tecnologia Agroalimentaries (IRTA), Fruitcentre, Parc Cientific i Tecnologic Agroalimentari (PCiTAL), Lleida 25003, Catalunya, Spain
[d] Institut des Géosciences de l'Environnement (IGE), CNRS, IRD, Univ. Grenoble Alpes, Saint-Martin-d'Hères, Grenoble, 38400, France

ARTICLE INFO

Editor: J.E. Fernández

Keywords:
Irrigation estimates
Irrigation Water Use
Soil Moisture
Remote Sensing
PrISM

ABSTRACT

Irrigated agriculture is the primary driver of freshwater use and is continuously expanding. Precise knowledge of irrigation amounts is critical for optimizing water management, especially in semi-arid regions where water is a limited resource. This study proposed to adapt the PrISM (Precipitation inferred from Soil Moisture) methodology to detect and estimate irrigation events from soil moisture remotely sensed data. PrISM was originally conceived to correct precipitation products, assimilating Soil Moisture (*SM*) observations into an antecedent precipitation index (API) formula, using a particle filter scheme. This novel application of PrISM uses initial precipitation and *SM* observations to detect instances of water excess in the soil (not caused by precipitation) and estimates the amount of irrigation, along with its uncertainty. This newly proposed approach does not require extensive calibration and is adaptable to different spatial and temporal scales. The objective of this study was to analyze the performance of PrISM for irrigation amount estimation and compare it with current state-of-the-art approaches. To develop and test this methodology, a synthetic study was conducted using *SM* observations with various noise levels to simulate uncertainties and different spatial and temporal resolutions. The results indicated that a high temporal resolution (less than 3 days) is crucial to avoid underestimating irrigation amounts due to missing events. However, including a constraint on the frequency of irrigation events, deduced from the system of irrigation used at the field level, could overcome the limitation of low temporal resolution and significantly reduce underestimation of irrigation amounts. Subsequently, the developed methodology was applied to actual satellite *SM* products at different spatial scales (1 *km* and 100 *m*) over the same area. Validation was performed using in situ data at the district level of Algerri-Balaguer in Catalunya, Spain, where in situ irrigation amounts were available for various years. The validation resulted in a total Pearson's correlation coefficient (r) of 0.80 and a total root mean square error (rmse) of 7.19 *mm/week* for the years from 2017 to 2021. Additional validation was conducted at the field level in the Segarra-Garrigues irrigation district using in situ data from a field where *SM* profiles and irrigation amounts were continuously monitored. This validation yielded a total bi-weekly r of 0.81 and a total rmse of −9.34 *mm*/14-*days* for the years from 2017 to 2021. Overall, the results suggested that PrISM can effectively estimate irrigation from *SM* remote sensing data, and the methodology has the potential to be applied on a large scale without requiring extensive calibration or site-specific knowledge.

1. Introduction

From a global perspective, irrigation has the largest water footprint among all human activities (Gleick, 2014), accounting for more than 70% of the total water withdrawals (Foley et al., 2011). The demand of irrigation steadily grew over the last decades (Wada et al., 2011) and it is expected to grow between 11% (Alexandratos and Bruinsma, 2012) and 19% Coates et al., (2012) by 2050, due to increasing food demand and the need to adapt to climate change (Wada et al., 2013; Hejazi et al., 2014; Fischer et al., 2007; Haddeland et al., 2014; Riediger et al., 2014).

* Corresponding author.
E-mail address: giovanni.paolini@isardsat.cat (G. Paolini).

https://doi.org/10.1016/j.agwat.2023.108594
Received 8 September 2023; Received in revised form 31 October 2023; Accepted 13 November 2023
Available online 22 November 2023

The quantification of irrigation amounts and its uncertainties is, therefore, a critical activity for water management, especially in semi-arid regions, where water is a limited resource. It is also fundamental to monitor the impact of irrigation on the global and regional hydrological water cycle (de Vrese et al., 2016; Ferguson and Maxwell, 2012; Harding and Snyder, 2012) and other earth system processes (McDermid et al., 2023).

Despite the importance of monitoring irrigation water use with precision, detailed information on irrigation amounts is often lacking worldwide (Folhes et al., 2009; Balasubramanya and Stifel, 2020; Foster et al., 2020; OECD, 2015). The main reason for this lack of information is the difficulty of measuring irrigation amounts locally using in situ sensors, as measurements are often either unavailable or not standardized. Furthermore, irrigation water abstraction sites are sometimes unknown. Remote sensing data could potentially address these shortcomings (Massari et al., 2021). These data are available at a global scale, at different spatial and temporal resolutions, and they can directly provide spatially distributed information on irrigation amounts.

Most of the previous works attempted to estimate irrigation amounts at different spatial scales assimilating remote sensing data into hydrological and land surface models. Various approaches proposed to assimilate observations of Soil Moisture (*SM*) Brocca et al. (2018); Kumar et al. (2015); Zaussinger et al. (2019), Evapotranspiration (*ET*) (Brombacher et al., 2022; Droogers et al., 2010; Kragh et al., 2023) or vegetation indexes from optical bands (Maselli et al., 2020; Olivera-Guerra et al., 2023; Hamze et al., 2023) to reproduce the actual (or ideal) water amounts supplied to the study area. An overview of the existing methodologies for irrigation estimation is presented in Massari et al. (2021) which sorts the different methodologies based on the remote sensing data used (sensor type and temporal resolution). Similarly, Foster et al. (2020) performed a meta-analysis over 41 previous research employing different methodologies, classified by the type of inputs used: thermal infrared, microwave *SM*, or crop coefficients from different spectral bands. The study concluded that remote sensing is an effective and low-cost solution to tackle the lack of information on irrigation amounts, but overconfidence in the results and a lack of proper validation of methodologies at different scales can be counter-productive and even harmful to general efforts on improving water management practices.

The majority of the approaches propose the assimilation of remote sensing data into a Land Surface Model (LSM) such as Noah (Nie et al., 2022; Modanesi et al., 2022, SURFEX (Escorihuela and Quintana-Seguí, 2016) and the Community Land Model (Sacks et al., 2009; Zhu et al., 2020; Yao et al., 2022). Other approaches proposed to estimate irrigation by closing the water balance equation using *SM* observations (Brocca et al., 2018, or comparing *ET* observations between irrigated pixels and non-irrigated areas (Brombacher et al., 2022), or between observed and modeled hydrological variables (Kumar et al., 2015; Zaussinger et al., 2019; Zhang and Long, 2021; Koch et al., 2020; Kragh et al., 2023; Peng et al. (2021) highlighted the need of using *SM* observations with a spatial resolution of at least 1 *km* to adequately describe irrigation practices.

Brocca et al. (2018) proposed to input *SM* observations into a simple soil water balance equation, modified from the SM2RAIN methodology, created for rainfall amounts correction (Brocca et al., 2014; Brocca et al., 2016). The approach proved to be successful in estimating irrigation at the district level, using different *SM* datasets as inputs (Dari et al., 2020; 2023) and coupling it with ET products (Dari et al., 2022). Nevertheless, the methodology showed increasing errors during rainier seasons and in discriminating between precipitation and irrigation amounts (Brocca et al., 2018; Dari et al., 2023; Brombacher et al. (2022) also proposed a simple approach based on the difference of actual *ET* between irrigated and natural hydrological similar pixels. The approach proved to be effective only for the case in which enough natural pixels were available in the study area, which is not always the case for intensively cultivated areas. Koch et al. (2020) and Kragh et al. (2023) proposed to compare modeled and observed *ET* values to estimate net irrigation at a spatial resolution of 1 *km* and 5 *km*, respectively. These approaches focused on the estimation of net irrigation, which is only a portion of the actual irrigation amount, corresponding to the evaporative loss. Zhang and Long (2021) proposed instead a methodology based on the difference between observed and modeled *ET* and root-zone *SM* to estimate actual irrigation amounts. The approach provides monthly irrigation amounts at 1 *km* resolution, without requiring any need for calibration. This methodology is based on the assumption that the difference between observed and modeled hydrological variables is due to irrigation. However, this assumption is not always valid, as the difference between observed and modeled variables can be due to different factors, such as model errors, errors in the input data, or errors in the observations. Moreover, the methodology is validated only at a yearly scale, and using spatially aggregated data at the regional level. This makes it difficult to assess the performances of the methodology at a finer scale, which is often the scale at which irrigation management decisions are made.

Recently, an increasing number of studies focused on irrigation estimates at the field level, made possible thanks to the availability of high-resolution remote sensing products, which allows finer spatial estimations but at the expense of a lower temporal frequency. Multiple studies investigated the feasibility of employing high spatial resolution/low temporal frequency data for irrigation estimation. Olivera-Guerra et al. (2018) used thermal-infrared data from the Landsat mission and vegetation indexes from the Sentinel-2 mission to constraint an FAO-56 water budget model and retrieve irrigation amounts at field scale. The approach proved useful in estimating total irrigation amounts over 5 irrigated fields in Marocco, but performances were not satisfactory at daily to weekly scale due to the low temporal resolution of the Landsat product. The authors concluded that satisfactory results could only be obtained with a temporal frequency of thermal data finer than 10 *days*, and also suggested that including an *SM* product would lead to improvements thanks to a better-defined topsoil condition. Similarly, Ouaadi et al. (2021) assimilated Sentinel-1 *SM* into an FAO-56 model. The study also showed how at least a 3-*day* revisit time is needed to correctly estimate irrigation amounts with this methodology. Modanesi et al. (2022) proposed to assimilate Sentinel-1 *SM* into the Noah-MP LSM coupled with an irrigation scheme (Niu et al., 2011; Ozdogan et al., 2010). The study concluded that the methodology can correctly estimate irrigation amounts at field level even though strong over- and under-estimation of irrigation amounts at a biweekly scale are present, probably due to large uncertainties in the model inputs. Moreover, the authors concluded that the temporal frequencies of Sentinel-1 observations, which were around 3 days in the study area, were not sufficient to detect all the irrigation events, and higher temporal resolution was needed. Finally, a study from Zappa et al. (2021) employed Sentinel-1 derived *SM* with a 500 *m* resolution using a simple water balance equation. The study showed results in line with the abovementioned literature: large underestimations were found due to missing irrigation events between two different satellite overpasses. The authors concluded that a temporal frequency of 3 days is needed to correctly estimate irrigation amounts at the field level. The general conclusion from studies focusing on irrigation retrieval at the field level was the need for *SM* observations at higher spatial and temporal resolution (which is a requirement also confirmed by Massari et al. (2021) in their review for irrigation quantification and timing methodologies at the field level).

This overview of state-of-the-art methods for estimating irrigation amounts highlighted some common shortcomings. Methods that employ *LSM* are often complex and require extensive calibration, which limits the generalization of the methodology. Moreover, This class of models requires a large amount of input data to correctly reproduce the state of the soil. Methods that employ remote sensing *SM* in simple water balance equations (such as SM2RAIN) are instead limited by the satellite *SM* product used, which is often available at low spatial resolution (around 1 *km*) or insufficient temporal frequency. Moreover, the

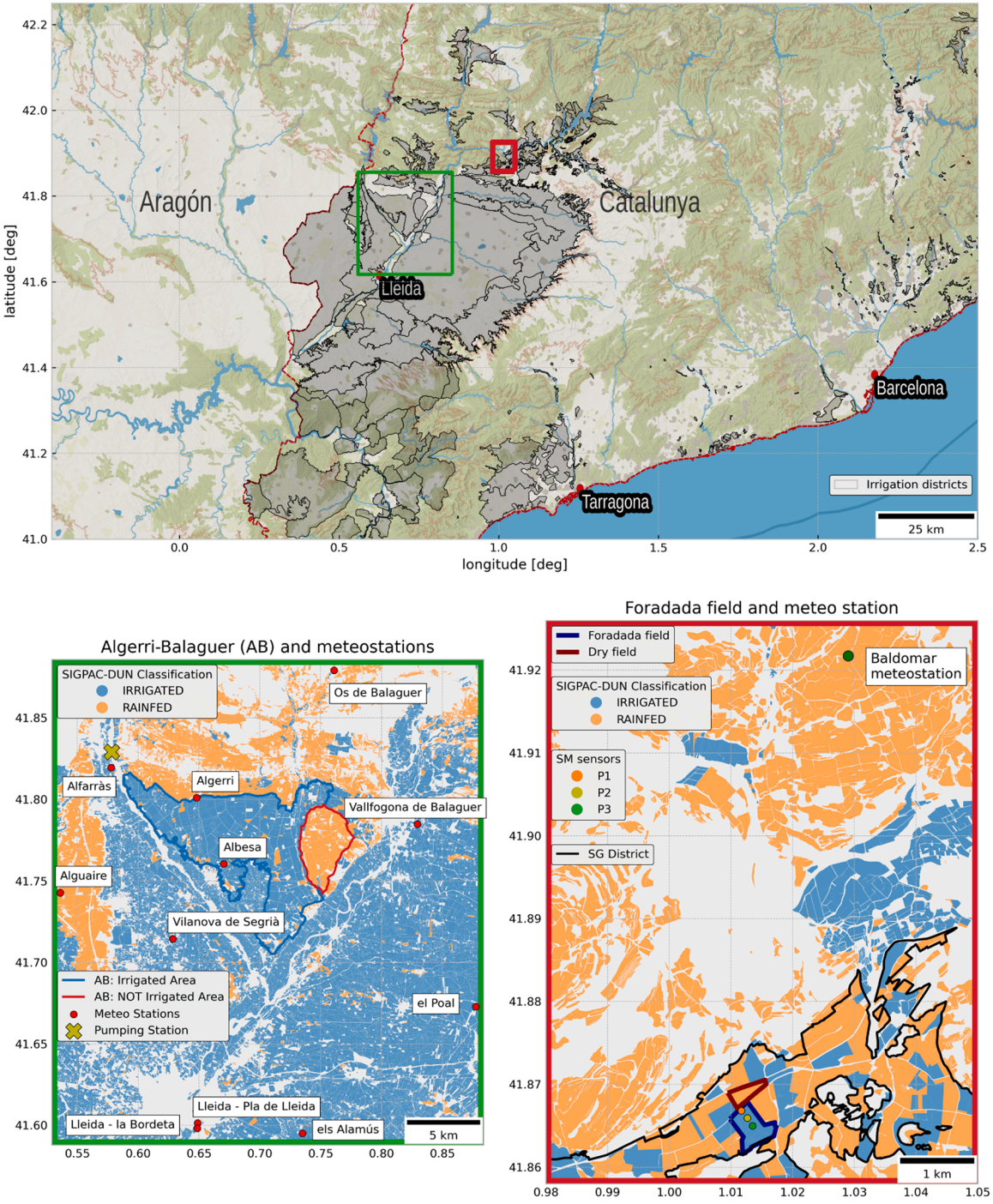

Fig. 1. On the top panel, a map representing the location of the two study areas, the Algerri-Balaguer irrigation district (green box) and the Foradada field (red box), which are located in the province of Lleida, in Catalunya, Spain. The main irrigation districts of the region are delineated. On the lower left panel, the Algerri-Balaguer irrigation district (in blue), on a map of irrigated and non-irrigated fields, from the SIGPAC-DUN administrative dataset. Meteo stations (red dots) and the water pumping station (green cross) are also shown. On the lower right panel, the Foradada field (in blue), on a map of irrigated fields from SIGPAC-DUN. The closest meteo station (Baldomar) is also shown (green dot), together with the three *SM* sensors installed in the field, and the border of the Segarra-Garrigues irrigation district (black line). The dry field taken as a rainfed reference is also shown (red line).

majority of the proposed methodologies do not provide uncertainty estimation.

In this study, we propose a novel methodology that builds on previous research and tries to overcome these limitations. The methodology is based on the PrISM (Precipitation inferred from Soil Moisture) (Pellarin et al., 2013) model, which is a simple soil water balance model that uses *SM* observations to estimate precipitation amounts. Similarly to SM2RAIN, the PrISM model is also originally developed as an inversion of *SM* observations to estimate precipitation amounts, but instead of a direct assimilation in the water balance equation, the method employs a particle filter assimilation scheme for *SM* into the Antecedent Precipitation Index Formula (API). This study proposes for the first time to adapt this methodology to estimate irrigation amounts instead of correcting precipitation amounts. Three main modifications to the algorithm are introduced in order to adapt the methodology to irrigation estimation and to overcome the limitations of previous methodologies: *i*)

a self-calibration process is performed in adjacent non-irrigated agricultural areas, to automatically retrieve the model's parameters. *ii*) Realistic assumptions on irrigation frequency (based on the irrigation system installed in the field) are used to mitigate the underestimation effect of low temporal frequency (around 6 days) *SM* observations. Previous studies tried to mitigate this effect by directly introducing precise information on irrigation timing, which is very difficult to obtain; *iii*) the model provides a simple estimation of uncertainties, based on the possible timing of the irrigation event between two *SM* observations. This provides additional details on the performances of the model and allows for a better interpretation of the results.

A synthetic study is carried out to assess the performance of the model in a controlled environment and to evaluate the novelties introduced by this methodology. The PrISM methodology is then tested over two different study areas, at the district and the field level, using actual satellite *SM* products with different temporal and spatial scales. At the district level, daily *SM* from SMAP disaggregated at 1 *km* using *S3 LST* was used over the 2016–2018 period. At field level, 6-*day SM* from SMAP disaggregated at 100 *m* using Landsat-7, Landsat-8 and Landsat-9 *LST* is employed. These two applications allow to study the effect of low-resolution/high-frequency or high-resolution/low-frequency *SM* products for the retrieval of irrigation amounts. Calibration is performed on the study area by selecting adjacent drylands, assuming that they have similar soil types and meteo conditions. The results are then validated using in situ irrigation data, and the performances of the model are discussed.

2. Study areas

This study proposes the application of the PrISM methodology for irrigation estimation at different spatial scales: district and field levels. Fig. 1 shows the location of the two study areas, the Algerri-Balaguer irrigation district and the Foradada field at the Segarra-Garrigues irrigation district, both located in the province of Lleida, Catalunya, Spain.

2.1. District level: Algerri-Balaguer

The Algerri-Balaguer irrigation district is located north of Lleida in Catalunya, Spain, and has an area of approximately 71 km^2. The region has a semi-arid climate, with total precipitation amounts of around 420 *mm* and around 72 rainy days (for the years from 2017 to 2021). The consolidated irrigation infrastructure brings water from the Pyrenees mountains, located northeast of the irrigation district, to the channel system that reaches individual fields. The area is ideal for studying the performances and the application at a large scale of this methodology. The main reasons are that *i*) the area has an irrigation monitoring system, in place since 2010, providing values of water flowing through the main pump at a daily scale for the district. The average cumulative amounts of irrigation for the period 2017–2021 correspond to 540 *mm*/*year*. Moreover, *ii*) the district borders a large non-irrigated agricultural area, which is close enough to share the same meteorological conditions and it is very useful to test the null hypothesis on the estimation of irrigation (it can give a clear estimate of any residual bias of the model). Fig. 1 shows the Algerri-Balaguer irrigation district on the lower left panel (blue line) together with the adjacent non-irrigated area (red line), the location of the pumping station (green cross) and the meteo stations (red dots). As shown in (Olivera-Guerra et al., 2023), the majority of the area is irrigated (75%) with sprinkler or drip irrigation. The majority of the fields are irrigated with sprinkler and cultivates double crops: barley in winter and maize in summer. Trees are located in the southern part of the district and are mostly irrigated by drip techniques, requiring less irrigation amounts.

2.2. Field level: Foradada

A water flow meter together with three *SM* sensors is installed in a field near the village of Foradada (41.8656 *N*, 1.012 *E*), close to Lleida, in the Segarra-Garrigues irrigation district (Fig. 1). The irrigation district has been recently equipped with a canal system that feeds irrigation to the entire area, even though most of the farmers have not yet equipped their fields with irrigation systems, so the area is mostly rainfed (Fontanet et al., 2018). For this reason, the Foradada field is an interesting study area, since its soil conditions are very similar to surrounding areas in winter/spring when cultivation is mostly rainfed, but they strongly differ in summer, when the field is one of the few that are irrigated, and it is surrounded by drylands. The Foradada field is approximately 20 *ha*, equipped with a sprinkler irrigation system, and cultivated with double crops: cereals during winter/spring and maize during summer. A flowmeter was installed in the irrigation system and provided irrigation amounts for several consecutive years, from 2017 to 2021. *SM* sensors were installed in 3 different locations in the field, and monitored *SM* at different depths, even though measurements were only collected during the year 2017. The closest dryland field is selected for the calibration of the PrISM methodology and it is visible in red in the lower right panel of Fig. 1.

3. Materials

3.1. Soil moisture

For this study, observed remote sensing *SM* is assimilated in the PrISM methodology to estimate irrigation amounts. To reach the adequate spatial resolution for analysis at the district and field level, DISPATCH (Merlin et al., 2012; Molero et al., 2016) was used to disaggregate the passive microwave *SM* product from SMAP (Entekhabi et al., 2010. Previous studies proved that both the original *SM* product from SMAP (Lawston et al., 2017) and the DISPATCH disaggregated product are capable of detecting the irrigation signal (Escorihuela and Quintana-Seguí, 2016). The original L3 enhanced *SM* product from SMAP is delivered at 9 *km*, and it is then downscaled to 1 *km* for the district-level study using MODIS optical and thermal data. Results at district scale produced using DISPATCH *SM* at 1 *km* are presented in 5.2. For the filed-level study, the 100 *m* product is retrieved from a disaggregation of the SMAP *SM* using Landsat optical and thermal data, which has a 100 *m* resolution. Results at field scale produced using DISPATCH *SM* at 100 *m* are presented in 5.3. Details about the DISPATCH methodology used can be found in (Merlin et al., 2013), where disaggregation of SMOS data is proposed with both thermal products at 1 *km* and 100 *m*. The only variation applied for this study was the use of a vegetation extension version of DISPATCH, which overcomes the limitation of disaggregating *SM* over areas with high Normalized Difference Vegetation Index (*NDVI*), by using the Temperature Difference Vegetation Index (TDVI) instead of the Soil Evaporative Efficiency (SEE) as a disaggregation parameter, as described in Ojha et al. (2021).

3.2. Meteorological data

For the district-level and field-level studies, meteorological data were retrieved from the Catalan meteorological network, which is openly accessible (https://ruralcat.gencat.cat/web/guest/agrometeo.estacions). Hourly air temperature and precipitation were retrieved from these meteo stations for the years 2017–2021. For the district-scale analysis, even though the nearby stations showed very similar values, the data were spatially distributed into the same grid and projection as the observed DISPATCH *SM* data at 1 *km* using the nearest neighbor approach (using the kd-tree algorithm (Maneewongvatana and Mount, 1999). Eleven of the closest stations were used to create this product, and they are identified in the lower left panel of Fig. 1. For the analysis at the field level, the data from the Baldomar meteo station was used, since it is the closest station to the Foradada fields, located approximately at a 6 *km* distance.

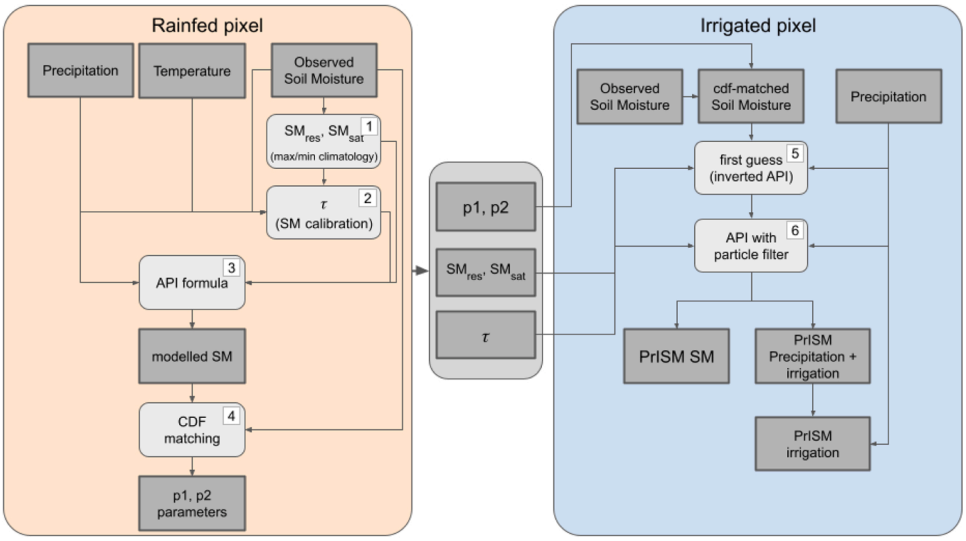

Fig. 2. Flowchart of the methodology. Data from the rainfed time series are used to retrieve the main parameters of PrISM (left side of the flowchart). These parameters are then applied to the irrigated pixel and irrigation amounts are retrieved (right side of the flowchart). The main steps in the processing pipeline are numbered from 1 to 6.

3.3. In situ irrigation data

In situ irrigation data are available as cumulative values for the entire district of Algerri-Balaguer. The infrastructure built for irrigation in the area delivers water from the Pyrenees mountains through constantly monitored and measured canal systems. Available data at daily resolution are openly accessible from the Automatic Hydrologic Information System of the Ebro river basin (SAIH Ebro). These data are then processed to account for losses due to drainage, pipe leaking and evaporation, corresponding to 5.8%, as proposed by (Olivera-Guerra et al., 2023) and weekly aggregated to account for any delay from the measuring date to the supply of irrigation to the soil. Finally, the data are converted from m^3 to mm by dividing it by the area of the district, corresponding to 70.79 km^2, as in (Dari et al., 2020). For the field-level study, irrigation data for the years from 2017–2021 were available from a flowmeter directly installed in the irrigation system of the Foradada field.

4. Methodology

The PrISM methodology (Pellarin et al., 2020; Pellarin et al., 2013) was originally designed to correct precipitation amounts using remotely sensed *SM*. The method employs a simple soil moisture/precipitation model which is a slight modification of the Antecedent Precipitation Index (API) and a particle filter assimilation scheme to ingest these *SM* observations. The approach proposed in this study follows the same structure of the classical PrISM, even though some additional steps are added in the processing pipeline. The main change proposed is the use of two sets of inputs, extracted from two different adjacent areas, irrigated and rainfed respectively, with the assumption that they share similar meteo conditions and soil types. Data coming from the rainfed area is used for calibration, to estimate the main parameters of PrISM, which are then used to retrieve irrigation amounts coming from the irrigated pixel. The methodology is described in detail in the following sections.

Fig. 2 visualizes and enumerates the main steps of the proposed methodology. In the first half of the process, on the rainfed pixel, the three main parameters of the API formula are retrieved (steps 1 and 2), and the API formula is then applied to the precipitation data from the rainfed pixel (step 3) to create a modeled SM. This modeled *SM* is then compared with the observed SM, to retrieve the two parameters for the CDF-matching, $p1$ and $p2$. In the second half of the process these parameters are applied to data coming from the irrigated area: a first guess of irrigation amount from the observed *SM* is computed (step 5), using the inverted API formula. This first guess is then used as input for the classic PrISM formulation and it is corrected to finally have a precise estimation of irrigation and precipitation amounts (step 6), from which the irrigation profile is retrieved by subtraction with the initial precipitation. In this study, the PrISM algorithm was designed using the Python programming language, version 3.9, and is freely available on the GitHub website (https://github.com/Giov-P/PrISM).

4.1. API formula

The API is a simple semi-empirical model used to reproduce soil water dynamics using time series of precipitation as input. API is widely used in rainfall-runoff applications to parameterize the *SM* conditions (Sittner et al., 1969; Descroix et al., 2002). In its initial formulation, it provides a proxy of the surface *SM* using as inputs a single precipitation observation and the parameter τ, which controls the soil drying-out velocity. This study employs the API formulation proposed by (Pellarin et al., 2020), which improves the accuracy of the formula by constraining the *SM* between two extreme values, representing the residual and saturated *SM* conditions. Additionally, the new API formula directly estimates volumetric *SM*, expressing it in m^3/m^3, instead of mm. The API is formulated as follows:

$$SM_t = (SM_{t-1} - SM_{res}) \cdot e^{-\frac{\Delta t}{\tau}} + (SM_{sat} - (SM_{t-1} - SM_{res})) \cdot \left(1 - e^{-\frac{P_t}{d_{soil}}}\right) + SM_{res} \quad (1)$$

Where SM_t is the Soil moisture at time t in $[m^3/m^3]$ retrieved from the precipitation P_t at time t, expressed in $[mm]$, the soil moisture SM_{t-1} at time $t-1$, the drying-out velocity τ expressed in $[h]$, the saturated and residual soil moisture values SM_{res} and SM_{sat}, the soil thickness of the soil moisture d_{soil} expressed in $[mm]$ and the interval of time between two observations Δt, expressed in $[h]$.

In the original formulation of the API, the only parameter that presents a spatio-temporal variability is τ, derived from the air temperature T, while SM_{res} is spatially varying (following a temporal average of *NDVI* and T) and d_{soil} also varies spatially, following a sigmoid function.

In this study, a data-driven approach was employed. The two parameters SM_{res} and SM_{sat} are determined for each pixel according to the maximum and minimum values of each time series of observed *SM* (step 1 of Fig. 2), d_{soil} is set constant to 50 $[mm]$, given that it is the average soil depth at which observed *SM* is provided. Following a sensitivity

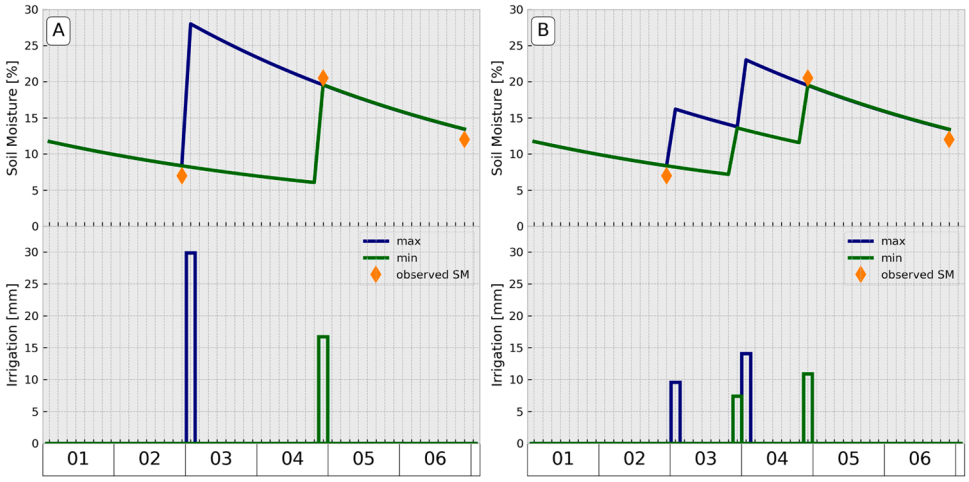

Fig. 3. Visualization of the temporal downscaling approach. In order to constrain the timing of the irrigation events, two scenarios are elaborated. The "maximum estimation" scenario assumes that irrigation occurs right at the beginning of the temporal window where the event is detected, while the "minimum scenario" places the event right at the end of the temporal window. Using these approaches allows constraining the irrigation amounts between these two retrieved values. On the left (A), an example of the max and min scenario without any constraint on irrigation frequency. On the right (B), the constraint on daily irrigation amounts is applied to the "max" and "min" scenarios.

study over the API parameters, τ was found to be the most sensitive parameter, with the largest impact on the modeled *SM*. For this reason, calibration of this parameter is performed based on the best fit between the model climatology and observed SM.

As detailed in Pellarin et al. (2020), in addition to the calibration of the τ parameter, a CDF-matching procedure is performed before assimilating the observed *SM* data into the model using the particle filter. The CDF-matching parameters are calculated exclusively between the modeled and observed time series of the rainfed pixel and the retrieved parameters are successively applied to the irrigated time series. The matching is performed using a linear fitting of the observed data against the modeled data, following the procedure illustrated by this formula:

$$SM_{CDF,obs} = p_1 + p_2 \cdot SM_{obs} \tag{2}$$

with $p_2 = \frac{\sigma_{API}}{\sigma_{obs}}$ and $p_1 = SM_{obs} - p_2 \cdot SM_{API}$.

The calibration of τ and the CDF-matching procedure are only computed on rainfed areas, where *SM* is only driven by precipitation, thus observed and modeled *SM* ideally represent the same evolution. Limiting this step to rainfed-only areas is particularly important since it avoids removing the observed irrigation signal that would occur if performing the CDF-matching over an irrigated pixel (Kumar et al., 2015; Jalilvand et al., 2023). As explained in this section, the proposed methodology includes both a calibration step and a CDF-matching procedure, which can be considered a second (fully empirical) calibration. This choice is justified by the different functions that these two steps serve: calibration of the API parameters is used to remove any bias between the modeled and observed *SM* time series, but it only affects the mean of the bias, while the CDF-matching procedure is used to remove any bias in the variance. The need for CDF matching is then justified by the fact that the API model is a simplification of the soil water balance equation, and it does not account for all the processes that affect the soil water dynamics. The two steps are performed sequentially, and the calibration of the API parameters is performed first, to avoid any bias in the CDF-matching procedure.

4.2. First guess

The API formula is used in steps 3 and 6 of the methodology proposed in Fig. 2, while an inverted API formula is used for step 5, to retrieve a first guess of precipitation and irrigation from observed *SM*. The inverted API formula is the following:

$$P_t \& I_t = -d_{soil} \cdot log\left(1 - \frac{(SM_t - SM_{res}) - (SM_{t-1} - SM_{res})e^{-\frac{\Delta t}{\tau}}}{(SM_{sat} - (SM_{t-1} - SM_{res}))}\right) \tag{3}$$

This direct inversion of the observed *SM* into precipitation and irrigation only provides a first guess and not a precise amount, since it does not account for errors related to the simplification introduced by the use of the API model and the intrinsic errors from the observed SM. Nevertheless, retrieving this first guess allows us to overcome one of the main limitations of the PrISM methodology, which is the inability to create precipitation (or irrigation) events (Pellarin et al., 2020).

In order to improve the quality of the first guess, a preprocessing step is applied before the ingestion of this first guess into the standard PrISM model. This preprocessing step involves the removal of all the negative estimation of precipitation and irrigation amounts, which are automatically set to 0, plus a temporal downscaling from the resolution of the observations (usually in the order of days, when the *SM* observations are retrieved from satellite products) to the resolution of the precipitation dataset (which is in the order of hours).

Temporal downscaling is a particularly important step in this methodology. This step is needed to have the same temporal frequency between irrigation (which is retrieved from inverted *SM* with a temporal resolution usually in the order of days) and precipitation (which has a higher temporal resolution, in the order of hours). Once an irrigation event is detected between two *SM* observations, the precise timing at which the irrigation event occurs remains unknown, and some design choices are needed to constrain this uncertainty. Two different scenarios are retrieved from the downscaling: one scenario where irrigation is placed at the beginning of the temporal window where the event is detected, and the second scenario where irrigation is placed at the very end of the temporal window, happening at the same time of the observed *SM*. The first scenario is here called the "maximum scenario" since it leads to the maximum possible estimation of irrigation amounts, as shown in Fig. 3. In this scenario, the largest amount of water is needed, because of the largest drying-out period that elapses between the irrigation events and the observed *SM*. The second scenario is exactly opposite to the first one and places the irrigation events right at the same time when the *SM* is observed. This is a "minimum scenario" since it leads to the least amount of estimated irrigation. In this scenario, the irrigation amount instantly drives the *SM* level observed, and there is no drying-out period. Fig. 3a shows these two scenarios and the modeled

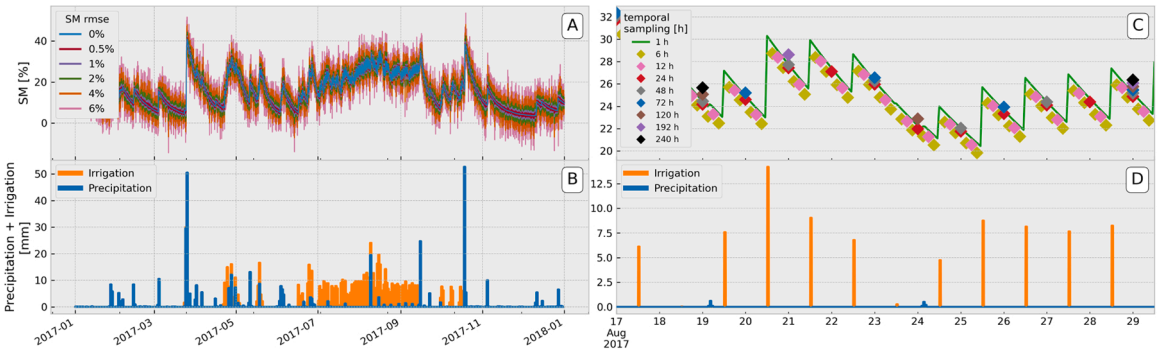

Fig. 4. Visualization of all the different *SM* profiles used for the synthetic study. (A) shows the *SM* profile with different noise levels, (B) shows the precipitation and irrigation amounts from in situ data taken from the Foradada field, which are used to build the synthetic observed *SM* profiles using the API formula. (C) shows different temporal samplings applied to the *SM* profile to reproduce the lower availability of *SM* from satellite data, while (D) shows the corresponding irrigation and precipitation for the period visualized.

SM derived with the PrISM approach. The irrigation amounts retrieved from these two extreme scenarios lead to define an empirical uncertainty of the estimated irrigation amount since the real value will ideally be contained in between these two estimations. Instead of using these two extreme scenarios, a more straightforward approach would be to aggregate the initial precipitation to the *SM* temporal frequency and estimate irrigation with the same temporal resolution. However, this approach would limit the quality of the retrieved irrigation amounts, since only one irrigation amount could be retrieved between each *SM* observation, not allowing to estimate uncertainties. Furthermore, the temporal aggregation would implicitly assume a constant and continuous amount of irrigation or precipitation between two *SM* observations, which is not always the case. Nevertheless, in case Precipitation is not available at a higher temporal resolution than *SM*, this approach could still be valuable to have a rougher estimation of irrigation amounts.

Fig. 3b shows an adaptation of the methodology to introduce an additional constraint on the irrigation timing: when observed *SM* data comes with a larger frequency than 24 h and an irrigation event is detected, it is assumed that multiple events are present in the window between these two observations, and they are distanced 24 h apart. The max and min scenarios are considered in this case as well. This constraint is applied under the regime of sprinkler irrigation, which is a type of irrigation that follows this daily frequency, while for more traditional irrigation systems, e.g. surface irrigation, the frequency is around once every two weeks with large amounts, so this constraint is not applied. This study focuses on an area where sprinkler irrigation is majorly used, so the constraint on the daily frequency is applied.

4.3. Particle filter

A particle filter assimilation technique is used to assimilate *SM* observation into the API model. Román-Cascón et al. (2017) demonstrated how introducing this assimilation scheme is advantageous for hydrological models, especially for the simple API model. Particle filter is advantageous compared to the class of assimilation techniques derived from the Kalman filter since it does not assume a Gaussian probability distribution of the prior sample, and the observation can be adapted to any non-linear and non-Gaussian application (Gordon et al., 1993; Moradkhani et al., 2005), which is most suitable for *SM* assimilation (Crow and Loon, 2006).

The particle filter methodology adopted in this study is derived from Pellarin et al. (2020), which follows the particle filter theory for *SM* assimilation proposed by Yan et al. (2015). As a first step, random stochastic perturbations are applied to the first guess of precipitation and irrigation amounts. This perturbation is created by multiplying these amounts by a set of 300 factors that vary uniformly between 0 and 2. Secondly, the amounts of irrigation and precipitation that are perturbed with the set of 300 factors, are then forced into the API formula to retrieve a final set of perturbed modeled *SM* time-series. Consequently, the assimilation of observed *SM* is performed every time 5 consecutive observations are available: in this window, the modeled *SM* set is evaluated against the observed *SM* through minimization of the total *rmse* and only the 30 factors leading to the smallest *rmse* are averaged together to retrieve a final value for the particular window. The same process is then applied to the next set of 5 observations, in a rolling window fashion, so that for each observation 4 factors are retrieved and averaged together. The final retrieved factor is finally applied to the first guess of precipitation and irrigation, to have a final corrected amount.

After the particle filter data assimilation, the last step involves separating the amount of precipitation from irrigation in order to obtain the final product. This final procedure is performed by removing all the precipitation events from the final time series, by setting to zero the amount of irrigated water in case a precipitation event was originally present in the dataset.

5. Results and discussion

5.1. Synthetic study

This synthetic study is performed to assess the performance of PrISM in a controlled environment. Real data from one year of precipitation and irrigation are retrieved from the in situ data available in the Foradada field. From these data, a synthetic *SM* profile is created using the API formula, all the parameters needed were retrieved from air temperature values and average *NDVI*, using the formulas proposed in Pellarin et al. (2020). A comprehensive number of tests are performed modifying this synthetic *SM* profile to adapt it to realistic scenarios. Three variations are introduced: the addition of white noise to simulate instrumental error from the observed *SM*, a variation of the temporal resolution of the data, a reduction in the frequency of available *SM*, and finally a variation of the spatial resolution of the data, which is simulated by changing the different percentage of irrigation present in the pixel detected by the observed *SM*. All the different synthetic *SM* profiles are successively assimilated into the PrISM model to retrieve the amounts of precipitation and irrigation. The performances of the model are evaluated in terms of the total error of estimated precipitation and irrigation, and the correlation between the estimated and the real daily irrigation amounts.

Fig. 4 visually presents the *SM* profiles used for the synthetic study and the precipitation and irrigation time series used as inputs to create the *SM* profiles and to evaluate the performances. Fig. 4A and C show *SM* from different noise levels and temporal frequencies. These *SM* profiles are retrieved from the distribution of precipitation and irrigation

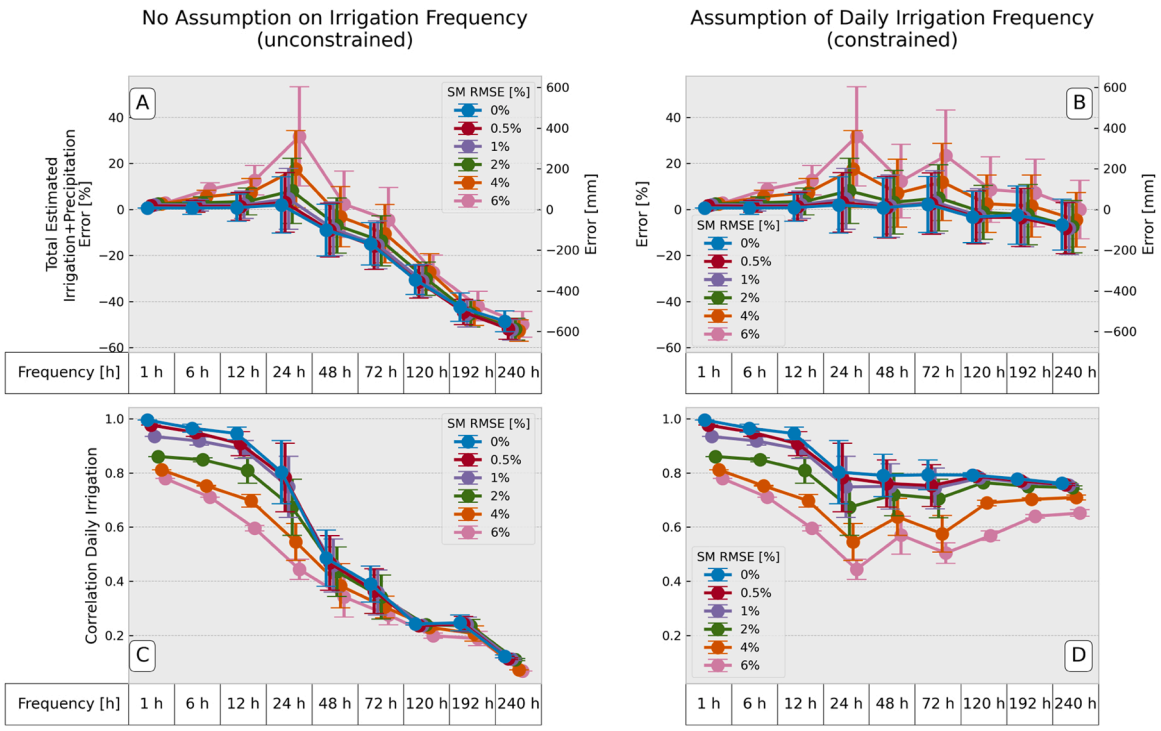

Fig. 5. Results from the synthetic study that shows the performances of PrISM in terms of total error from retrieved precipitation+irrigation (first row) and correlation of daily irrigation (second row). Results are presented for two different PrISM configurations: with no constraint (left column) and constraining irrigation events to a daily frequency (right column) which corresponds to assuming a modern irrigation practice, e.g. sprinkler irrigation. All the plots show the performance degradation when decreasing the *SM* temporal frequency (expressed in hourly frequency *h* along the x-axis), and when adding noise to the signal, as shown for the different lines described in the legend. Error bars represent the variation of values between the "maximum" and "minimum" scenario.

presented in Fig. 4B and D. The *SM* profiles created from different percentages of irrigation are here omitted but results from those tests are shown in the appendix A.

Fig. 5 visualizes the results from the synthetic study for 2 different configurations of the PrISM methodology, which correspond to the unconstrained version (left column) and a version where a modern irrigation system is assumed, so irrigation is created with a daily frequency (right column). Each plot shows the performances of PrISM when decreasing the temporal frequency of *SM* observations (expressed in *h* in the x-axis) and when increasing the noise (represented by the different colors of the curves). Error bars are retrieved from irrigation amounts corresponding to the maximum and minimum scenario. Results are presented in terms of the total error of estimated annual precipitation and irrigation in the first row of Fig. 5, while the second row shows results in terms of daily irrigation correlation (expressed by the Pearson's r coefficient) between in situ irrigation and irrigation estimated by PrISM.

Analyzing Fig. 5A, it can be noticed that the error on the total amount of precipitation and irrigation grows towards negative values (underestimating the total amounts) when the temporal frequency of the *SM* observations decreases. This underestimation is caused by increasing amounts of missed irrigation events, especially with observations at a temporal frequency lower than 24 *h*, since irrigation is performed daily in this simulation and not all events can be detected if *SM* observations are not available daily. This explains the sharp increase in underestimation of the total amounts after the 24 *h* temporal frequency of *SM* observations. On the other hand, increasing noise in the observed *SM* has the opposite effect of overestimating the total amounts. This is also easily explainable: higher noise leads to an increase of "false positives" irrigation events, created by the random fluctuation of the irrigation signal. These two trends partially compensate for each other in terms of the total error of precipitation and irrigation, but they both contribute to quick degradation of the correlation values (as it can be seen in Fig. 5B).

The right column of Fig. 5 shows results for the assumption of daily irrigation. This assumption distributes irrigation on a daily whenever an irrigation event is detected, which is a realistic assumption for modern irrigation practices, such as sprinkler irrigation, which usually happens with this frequency. Fig. 5B and C show how this assumption greatly improves the performances of PrISM, both in terms of error on the annual estimated amount of irrigation and precipitation and correlation of daily irrigation, proving that it is possible to mitigate the effect of limited availability of observed *SM* if information about irrigation practices is available. As it is noticeable from Fig. 5B, the error on the total amount of irrigation and precipitation shows the same degrading trend for the two configurations in the left and right columns, until it reaches the 24 *h* temporal resolution of observed *SM*. After this temporal resolution, values stabilize when using the assumption of daily irrigation. The same behavior can be observed in Fig. 5D, where the correlation flattens after the 24 *h* temporal frequency. It is also noticeable how correlation slightly improves when degrading the temporal frequency of *SM* profiles with a high noise content (above 2%). This is also reasonable since with the daily constraint the model is less dependent on the noisy *SM* profiles and performs slightly better when fewer observations are present because it also reduces the frequency of "false positive" detection.

Results for this synthetic experiment are in line with previous studies that proposed a similar approach, based on assimilating *SM* observations to estimate irrigation amounts. Filippucci et al. (2020) showed a daily correlation lower than 0.3 when decreasing the temporal frequency of the observation up to 120 *h*, and similarly, in Zappa et al. (2022) the correlation between retrieved and actual irrigation amounts decreased down to 0.4 for a temporal resolution of 144 *h* and a simulated irrigated quantity of 5 *mm*. These results are very well in line with what has been presented in Fig. 5C, where the daily correlation r is lower than 0.3 with higher temporal frequencies than 120 *h*.

Jalilvand et al. (2023) retrieved irrigation from a synthetic study

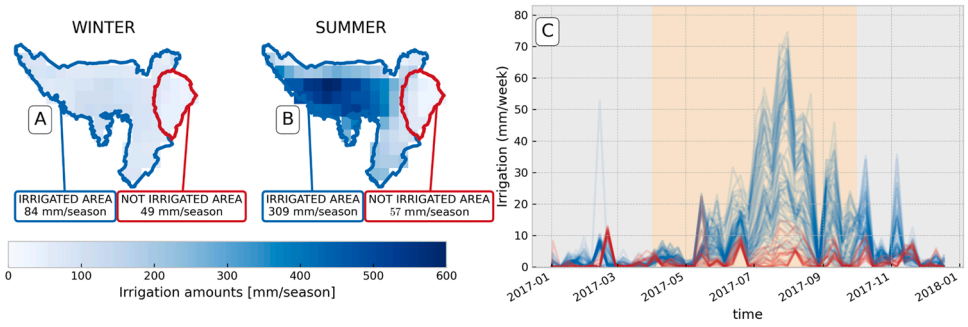

Fig. 6. Results from PrISM applied at the pixel level in the Algerri-Balaguer district and the adjacent dryland area. (A) shows the spatial distribution of the irrigation amounts in Algerri-Balaguer for the winter period (January to April and October to December of the year 2017). The borders of the irrigated and dryland areas are delineated in blue and red, and the total amount of irrigation is shown. (B) shows the equivalent maps for the summer season (April to October of 2017). (C) shows the irrigation time series retrieved for all the pixels inside the irrigated area (blue lines) and the pixels in the dryland (red lines). The orange background shows the summer period.

with fixed noise levels and 3 different temporal frequencies (1, 6, and 12-*day* temporal frequency), also showing a negative bias due to missing detected irrigation. Additionally, it shows how degradation due to lower temporal frequencies of observations can be avoided completely when irrigation timing is known (which is in line with the constrained results shown in Fig. 5B and D). Nevertheless, results from the synthetic study presented in this work, demonstrated how it is not strictly necessary to know the exact timing of irrigation events, but it is sufficient to know the irrigation frequency (e.g. daily irrigation) to avoid the degradation of the performances of PrISM.

5.2. District scale: Algerri-Balaguer

The PrISM model adapted for irrigation estimation is consequently applied to observed *SM* data at 1 *km* resolution, derived from the disaggregation through DISPATCH of SMAP *SM* gridded at 9 *km* with *NDVI* and *LST* from *MODIS* at 1 *km*. Given that the *SM* and precipitation variables across the dryland area are quite homogeneous, calibration results do not vary across the pixels in the area, so a single representative pixel from the dry-land area is selected to calibrate the parameters p_1, p_2, sm_{res}, sm_{sat}, and τ, following the procedure illustrated in Fig. 2. Nevertheless, the methodology can be easily extended to a larger area and multiple pixels, as long as the assumption of similar meteo conditions and soil types is valid. Following calibration, results are then produced for each pixel of the irrigated area of Algerri-Balaguer. Fig. 6 shows the results for the year 2017.

Fig. 6A and B shows the spatial distribution of the irrigation amounts for the winter and summer period of the year 2017. The red area represents the dryland area, while the blue area represents the irrigated area, and the average amounts of irrigation for the two areas and the two seasons are written in the respective boxes. It is possible to notice how the spatial distribution of the irrigation amounts correctly detects the irrigated and dryland areas, showing most of the irrigation amounts in "summer" for the irrigated areas, with values reaching 600 *mm* (blue textbox in Fig. 6B), which is an amount of irrigation expected in this area. Nevertheless, it is also possible to notice how a small amount of irrigation is also detected in the dryland area both in "winter" and "summer", with an average irrigation amount of around 50 *mm* for both seasons. This amount should be considered as an error of the model, irrigation is not practiced in this dryland area. This error is also visible in the time series of Fig. 6C, where the irrigation time series of the dryland area (red lines) shows some isolated irrigation events occurring both in winter and in summer. The fact that these events seem very homogeneous for all the drylands pixels (both in timing and amount) suggests that they are not real irrigation events, but they are most probably precipitation events that were not included in the Precipitation datasets used as input, and for this reason, are misclassified as irrigation.

Another interesting result from the spatial distribution of Fig. 6B is the difference in irrigation amounts between the northern and southern parts of the irrigated area. The northern part of the irrigated area shows a higher amount of irrigation, whilst the southern part generally shows lower amounts of irrigation. This can be explained by the different irrigation practices of the two areas: the northern part is mainly cultivated with double crops and irrigated by sprinkler systems, which requires a higher amount of irrigation, while orchard trees are mainly present in the southern part and they are subject to drip irrigation, which requires a lower amount of irrigation.

In order to evaluate the performances of the PrISM model at the district level, the results are compared with the in situ data available for the Algerri-Balaguer district. Fig. 7 shows the results for the years 2017–2021 and the performances of the model are evaluated against in situ data in terms of Pearson's correlation (r), rmse, and bias.

As illustrated in Fig. 7, PrISM shows a good correlation with the in situ data, with a total r equal to 0.80 for all the years, and oscillating between 0.79 (2018) and 0.87 (2020) when considering the single years. A slight underestimation of the irrigation amounts is present: the bias equals − 1.76 *mm/week* for the overall total, and it oscillates between − 3.64 *mm/week* (2017) and 0.43 *mm/week* (2020) for the different years. The model shows a good performance also in terms of rmse, with a total rmse of 7.19 *mm/week*, and between 5.06 *mm/week* (2020) and 8.81 *mm/week* (2017) for the single years. Generally, it can be seen that 2020 shows the best performances for all metrics, but it could be related to the smaller portion of the year used for the comparison. As a matter of fact, in situ data were not available for a relatively large period during the irrigation season, which could affect the metric computation for that year. Conversely, 2017 shows lower performances while being the only year with no missing periods. Nevertheless, the performances only slightly vary over the years and we can conclude that the total metrics are representative of the performances of PrISM in Algerri-Balaguer.

These results can be compared with previous works that developed different irrigation estimation techniques over the same area. Dari et al. (2020) firstly presented results on a district scale estimation of irrigation in Algerri-Balaguer for the year 2016 − 2017, showing a correlation coefficient r of 0.76 and a rmse of 6.11 *mm*/5-*days*, using DISPATCH *SM* retrieved from SMAP, as in this study. Additionally, Dari et al. (2022) reported for the same years a correlation coefficient r between 0.61 and 0.76 and a rmse between 6.11 and 8.14 *mm*/5-*days*, depending on the different dataset used, since multiple experiments were performed using *SM* and *ET* datasets at 1 *km*. When converting the results of our study to the same 5-*day* temporal resolution, a correlation r of 0.78 is found, and a rmse of 6.45 *mm*/5-*days* for the year 2017. These results show a slight improvement concerning these two previous studies, in terms of correlation r, while a similar rmse is found.

Dari et al. (2023) reported for the years 2016–2019 a correlation coefficient r equals to 0.78 and a rmse of 14.41 *mm*/14-*days* for the Algerri Balaguer district, using the SM2RAIN algorithm with *SM* from

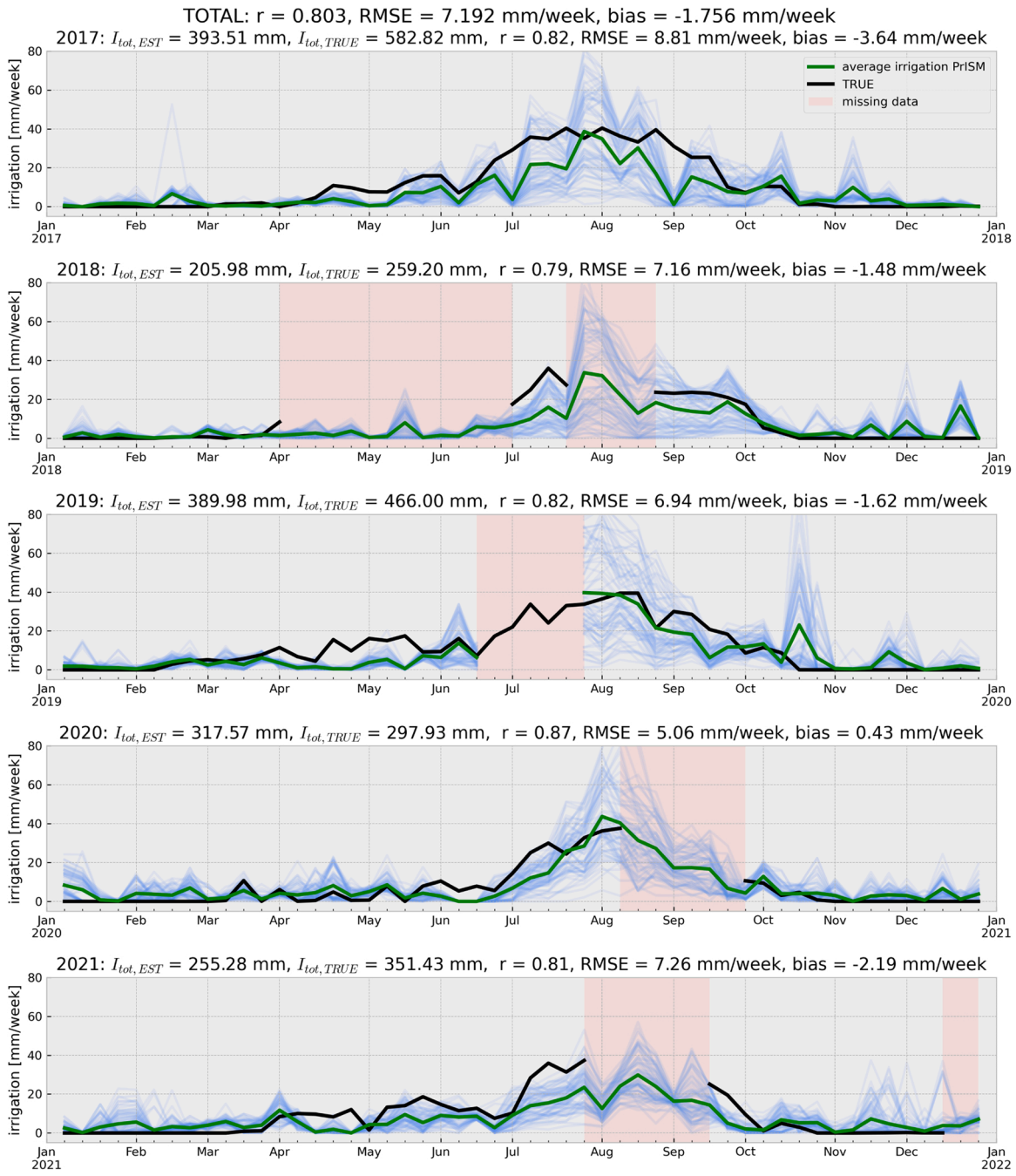

Fig. 7. Time series of irrigation retrieved from PrISM at the pixel level (blue lines) and average retrieved irrigation (red line) compared with in situ data (black line) for the Algerri-Balaguer district. The analysis shows the results from different years in terms of total irrigation amount observed ($I_{tot,EST}$) and from the insitu station ($I_{tot,TRUE}$), Pearson's correlation (r), rmse, and bias.

Sentinel-1. If converted to a 14-*day* period, the PrISM methodology shows higher performances, with a correlation r of 0.84 and a rmse of 12.16 *mm*/14-*days*. Nevertheless, it is important to notice that the results from Dari et al. (2023) are retrieved from Sentinel-1 *SM* at 1 *km*, which is a different dataset from the one used in this study. Additionally, the results from Dari et al. (2023) are retrieved after a calibration of the model using in situ data from the year 2019, which is not the case for the other studies that employed SM2RAIN, which fully rely on remote sensing data.

5.3. Field scale: Foradada

The PrISM model is also applied at the field level for the Foradada field, using the *SM* product from DISPATCH at 100 m. The model is calibrated with the same procedure described in Section 5.2, using the time series from a non-irrigated field very close to the Foradada field, as shown in the lower right panel of Fig. 1. The results are shown in Fig. 8.

Fig. 8A shows in purple the in situ *SM* and in green the PrISM *SM* between the maximum and minimum scenarios, which follows closely the observations from DISPATCH 100 *mSM*, depicted as orange diamonds. It is important to notice that the purple line that indicates insitu *SM* is not scaled with the green line representing *SM* built from PrISM, since in-situ data are not calibrated against the Dispatch remotely sensed *SM* assimilated by PrISM. Nevertheless, visual inspection reveals a good agreement between the trends of the two *SM* curves, which is a useful indicator of the goodness of the results. Irrigation is shown in Fig. 8B and

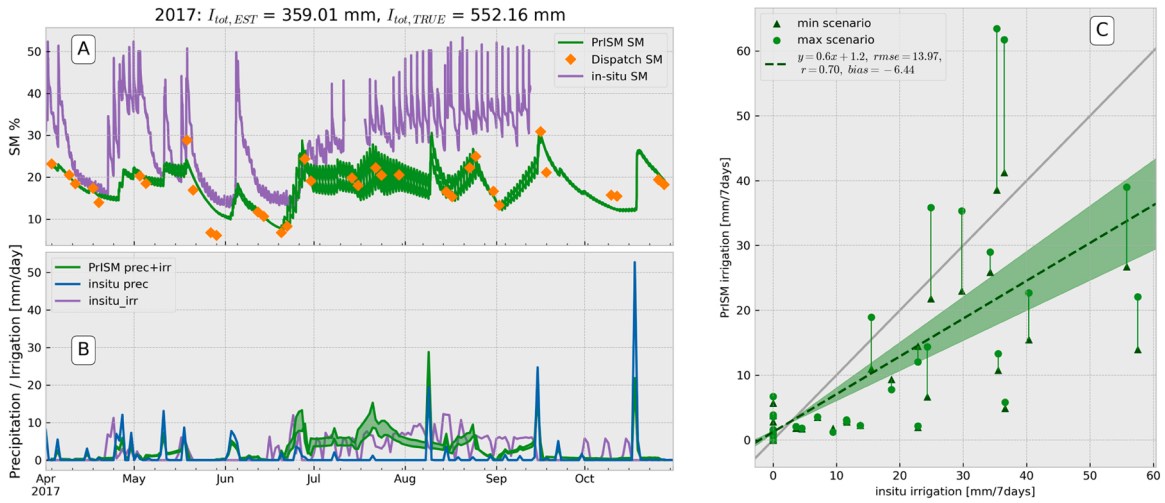

Fig. 8. Results of the PrISM model applied at field level for the Foradada field, using the *SM* product from DISPATCH at 100 m. The estimated ($I_{tot,EST}$) and real ($I_{tot,TRUE}$) amount of irrigation is shown in the figure title. (A) shows the time series of observed *SM* from DISPATCH (orange diamonds), the in situ *SM* at 5*cm* from capacitative sensors (purple), and the resulting *SM* curves from the PrISM approach for the minim and maximum scenarios (green lines). (Note that in situ *SM* is not calibrated against dispatch *SM*, hence the *SM* curves are not scaled.) (B) shows the time series of precipitation (blue line) from the closer meteo station of Baldomar, the in situ irrigation amounts (purple line), and the amounts of irrigation estimated by PrISM for the minimum and maximum scenarios (green lines). (C) shows the scatter plot between the weekly irrigation amounts estimated by PrISM for the maximum (circles) and minimum (triangles) scenarios and the in situ irrigation amounts. The legend shows the metrics extracted from this comparison (Pearson's correlation, rmse, and the slope and intercept of the linear relationship).

it is possible to notice how retrieved irrigation from PrISM (the green bands between the "maximum" and "minimum" scenarios) is generally in agreement with the in situ irrigation periods and amounts, in purple. It is noticeable that, for the month of July, the retrieved irrigation amounts are in close agreement with the in situ data, while there is a progressive underestimation of irrigation amounts during August, especially towards the end of the month and the start of September. This underestimation is caused by the drop in values of the DISPATCH *SM* at the end of August, suggesting a dry soil condition, which seems to disagree with the in situ *SM* measurements and irrigation amounts. This discrepancy highlights the need for precise (and frequent) *SM* observations in order to obtain a correct irrigation retrieval from PrISM, and showcases the impact that errors on multiple consecutive observations have on this estimation.

From a quantitative point of view, PrISM generally shows good performances when compared to in situ data. Fig. 8C shows the relationship between weekly irrigation amounts estimated by PrISM for the minimum and maximum scenarios and the in situ irrigation amounts. The legend shows the metrics extracted from this comparison (Pearson's correlation, rmse, and slope and intercept of the linear relationship). rmse corresponds to 12.61 *mm/week* for the maximum scenario and 7.93 *mm/week* for the minimum scenario, while the correlation corresponds to 0.69 for the maximum scenario and 0.70 for the minimum scenario. The slope of the linear relationship is 0.5 for the maximum scenario and 0.4 for the minimum scenario, while the intercept is 1.4 for the maximum scenario and 1 for the minimum scenario.

In situ irrigation amounts from the years 2018–2021 were also available for the Foradada fields, even though the *SM* sensors were removed from the field for the years following 2017. Fig. 9 shows the scatter plot between in situ vs. PrISM irrigation amounts. Time series of *SM* and irrigation retrieved from PrISM for these years are added in Appendix B.

Results from the year 2018 show the best agreement with in situ data, with a correlation of 0.84, an *rmse* of − 10.52 *mm/week*, and a bias of − 1.80 *mm/week*. The following years show lower performances, with a correlation of 0.66, 0.59, and 0.57, an *rmse* value of 17.95, 24.29 and 19.58 *mm/week* and a bias of − 7.40, − 4.07 and − 5.68 *mm/week* for 2019, 2020 and 2021 respectively. Generally, the metrics from these different years are quite consistent and they do not show a dramatic change. For the last three years, from 2019 to 2021, the lower performances can be attributed to gaps in the observed *SM*, with fewer available observations than in 2018, especially during the winter period. Additionally, in 2019 SMAP had a malfunctioning and was switched to safe mode from the 19^{th} of June to the 23^{rd} of July, making observations during that period unavailable.

Aggregated results for the years 2017–2021 show a bi-weekly correlation r of 0.81 and an *rmse* of 25.81 *mm*/14-*days* (as shown in Fig. B.5), which are in line with the results obtained at the district level, even if they show a degradation of the performance. As expected from the synthetic study, irrigation retrieved with PrISM at the field level shows an underestimation of the total irrigation amounts, mainly caused by the low temporal frequency of the observed *SM*, which is derived from Landsat *LST*, available at best every 8 days in cloud-free conditions. Nevertheless, the model shows a good correlation with the in situ data and seems to correctly reproduce the *SM* and irrigation profiles.

Compared with other studies performed at the field level using remotely sensed *SM*, PrISM shows better performances in terms of correlation and *rmse*, even though experiments were performed in different areas and with different datasets. Ouaadi et al. (2021) uses *SM* from Sentinel-1 data at field level to retrieve 15-*day* cumulated irrigated amounts, with a final correlation r of 0.64, an *rmse* of 28.7 *mm*/15-*days* and a bias of 1.9 *mm*/15-*days*. Zappa et al. (2021) also used Sentinel-1 data to detect irrigation events at field level, with a mean Pearson correlation r = 0.64 and a large variability of the bias, varying from 8 *mm/season* to − 98 *mm/season* for the different fields. Both these studies stress the importance of a higher temporal frequency of the *SM* observations, which is the main driver for improvements in irrigation amount retrieval. Brombacher et al. (2022) proposed a methodology to estimate irrigation amounts at field level from the difference in actual ET of an irrigated pixel against a "hydrological similar pixel", found in the surrounding natural areas. Results in the Ebro Valley (same study region of this work) were not statistically significant, since only a few areas were identified as hydrological similar pixels and they were quite distant from the irrigated fields. The authors proposed further studies to investigate the possibility of using non-irrigated agricultural pixels instead of natural areas, which is in line with the approach presented in this study.

In general, the methodology follows a similar development as the

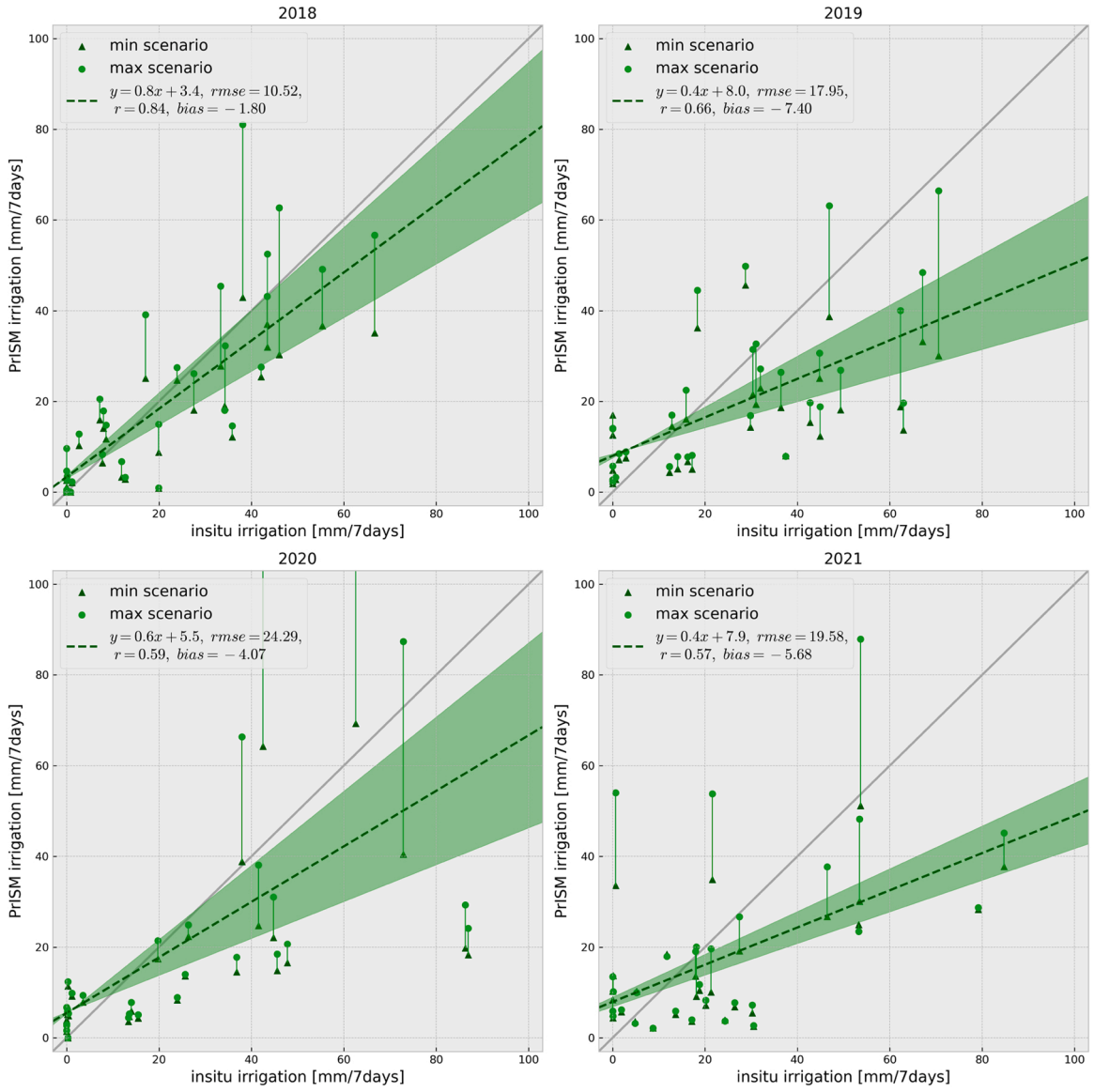

Fig. 9. Comparison between in situ and PrISM irrigation amounts during 4 different years (2018–2021) for the Foradada field. The maximum (circle) and minimum (triangle) scenarios produced by PrISM are shown. The dotted line represents the linear relationship from the average PrISM values. The green band is the interval of values between the linear relationship formed by the maximum and minimum scenarios. The legend shows the metrics (Pearson's correlation, rmse, and the slope and intercept of the linear relationship) extracted from the comparison between in situ irrigation and average PrISM values.

SM2RAIN algorithm Brocca et al. (2018); Dari et al. (2020), since they are both adapted from a precipitation correction approach employing *SM* observations into a simple model. One particular difference between these two methodologies is the use of a different modeling approach and data assimilation: while SM2RAIN uses the original water balance equation and directly assimilates *SM* observations into the model, PrISM uses the API formula and assimilates *SM* observations through a particle filter approach. The API formula proposed might be considered a solution to the water balance ordinary differential equation, as shown in Pan et al. (2003), which is an element of connection between the two models. Regarding the assimilation of *SM* into the model, the particle filter approach is more robust than the direct assimilation of *SM* into the water balance equation, since it takes into account observation uncertainties and effectively combines effecctively a physical model and successive observational data (i.e. this study employed a rolling window of 5 consecutive observations for each run of the particle filter). Additionally, this study also introduces the possibility of constraining the irrigation frequency to a daily frequency, as well as the creation of different scenarios for the irrigation amounts, which allows for the creation of a range of possible irrigation amounts. These two features are not present in SM2RAIN, but they can easily be added to it since they are model agnostic.

6. Conclusion

This study introduces a new methodology for estimating irrigation amounts based on PrISM (Precipitation Inferred from Soil Moisture). The methodology is lightweight and data-driven, capable of replacing complex LSM models with a simple API formula, coupled with a particle filter assimilation scheme while maintaining similar performances at different spatial scales. The proposed methodology only requires observations of *SM* and precipitation amounts, along with a few parameters that can be retrieved from these variables during a self-calibration step run over dry areas adjacent to the irrigated ones. Originally, the classical PrISM methodology was exclusively designed to correct precipitation amounts and did not allow for the creation of precipitation (or irrigation) events. However, this study demonstrates how it is possible to create precipitation and irrigation events by using a first guess of the *SM*

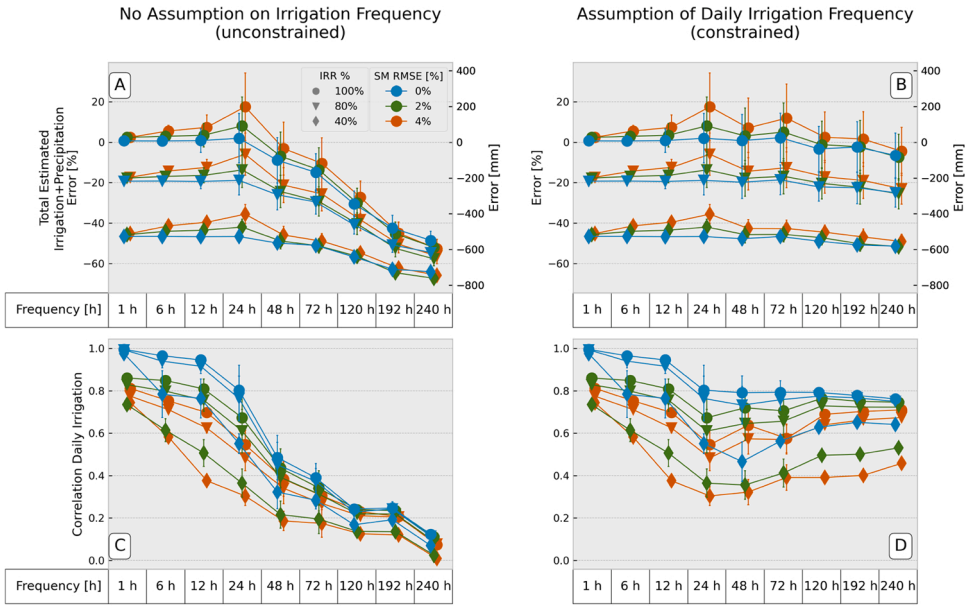

Fig. A.1. Same description as in Fig. 5, but for a synthetic study where the pixel is only partially irrigated and different percentages of irrigation are presented. The irrigation amount is not completely retrieved for irrigation percentages lower than 100% and there is a bigger underestimation (the irrigation signal is mixed with the signal from dryland).

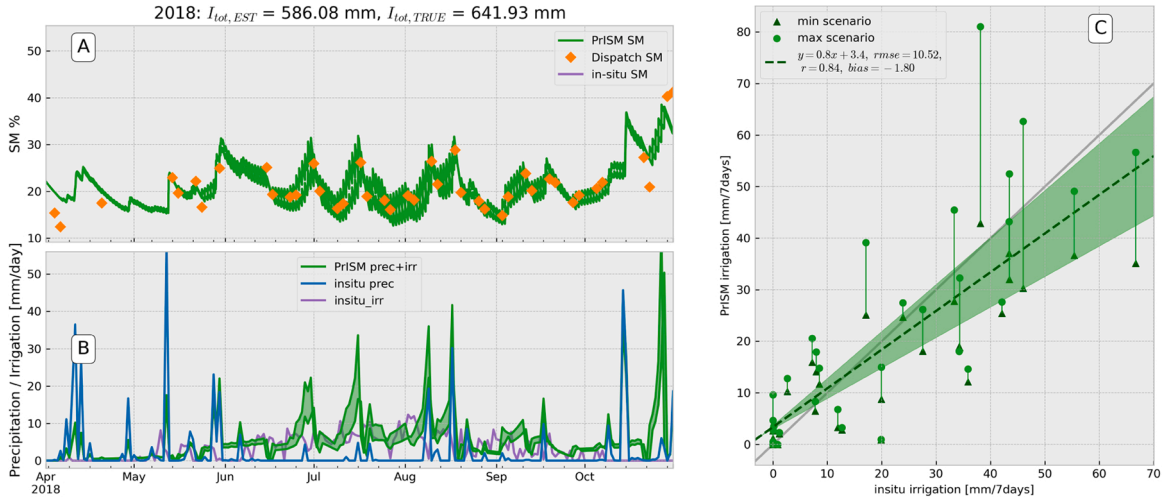

Fig. B.1. time series and scatter plot of soil moisture and irrigation amounts retrieved by PrISM for the Foradada field in 2018. Same description as in Fig. 8.

profile, derived from the inversion of the API formula, directly applied to observed data. Additionally, the methodology was adapted for irrigation estimation by i) adding a maximum and minimum scenario, allowing the creation of a range of possible irrigation amounts, and ii) introducing the possibility of constraining the irrigation frequency to a daily frequency, which is a realistic assumption for modern irrigation practices, such as sprinkler irrigation.

The results of the synthetic study demonstrated that constraining irrigation timing is beneficial when assimilating *SM* observations with low temporal frequency (lower than 72 *h*). This overcomes the limitation of high spatial resolution *SM* products, which are notably suffering from low temporal resolution. Using a constrained daily irrigation approach leads to a visible performance improvement when compared with the unconstrained approach.

PrISM was then successfully applied at the district scale using observations from the DISPATCH *SM* at 1 *km* product, showing similar or even better results than previous studies conducted in the same study area. Additionally, PrISM was applied at the field scale using DISPATCH *SM* at 100 *m*. The results demonstrated how the methodology can be applied at different spatial resolutions and temporal frequencies, ranging from 1 to 2 days at the district level to around 6 days at the field level. The performances obtained improve the current state-of-the-art in estimating irrigation amounts from remotely sensed *SM*.

In general, the methodology can be easily applied to large areas if an irrigation map is available as auxiliary information. This map is used to select the rainfed area and perform the calibration step. When applied at the field scale, it is also beneficial to provide the methodology with a map of irrigation systems, which is used to constrain the irrigation frequency (daily for modern irrigation systems such as sprinkler and drip, and biweekly for traditional flood irrigation systems). Maps of irrigation systems have been recently developed (Paolini et al., 2022) and could be applied to this methodology in future iterations over larger areas.

Future work should be directed towards studying the influence of different precipitation datasets on irrigation retrieval and assessing the uncertainties created by the use of remotely sensed meteorological data, which is expected to be considerable (Foster et al., 2020). For this study,

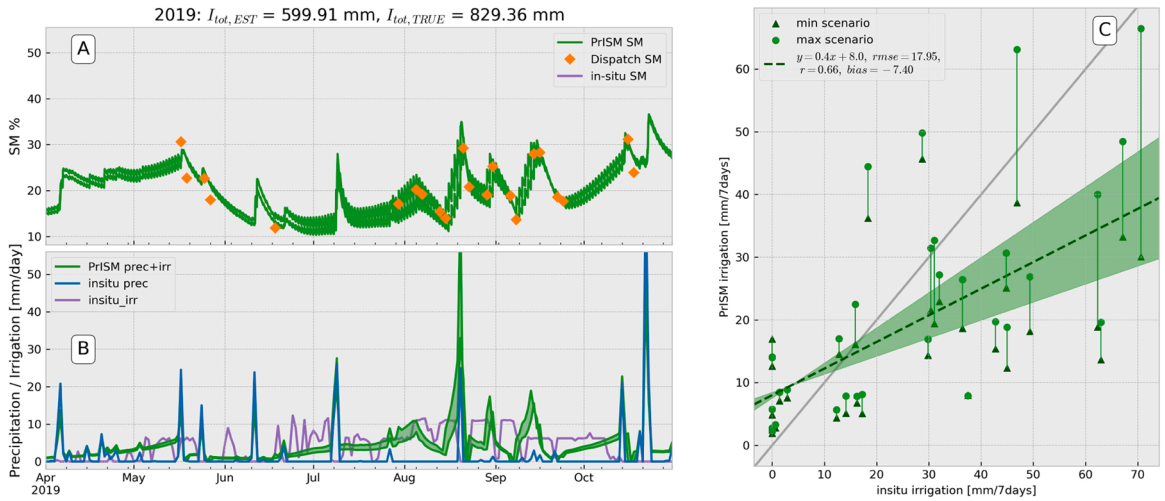

Fig. B.2. time series and scatter plot of soil moisture and irrigation amounts retrieved by PrISM for the Foradada field in 2019. Same description as in Fig. 8.

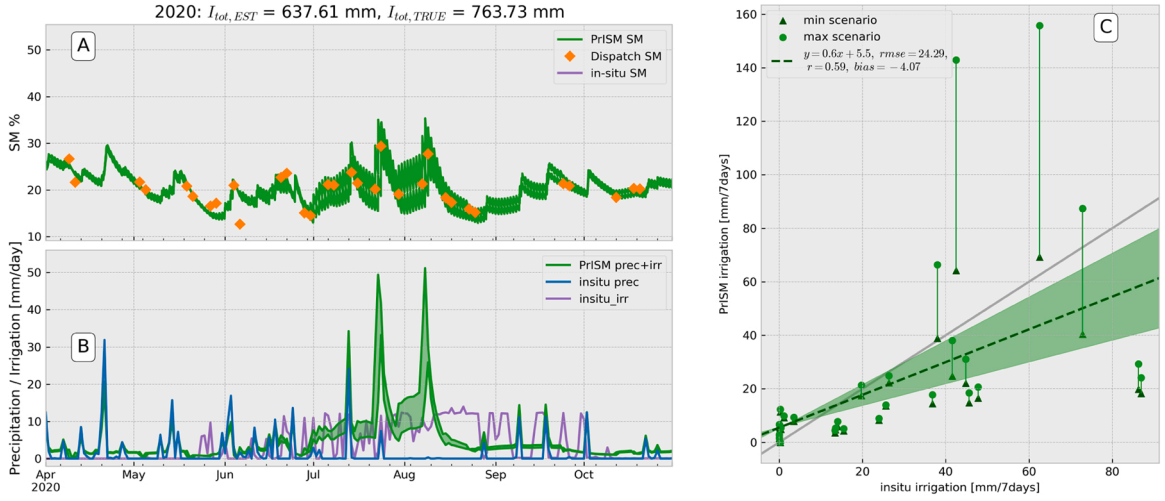

Fig. B.3. time series and scatter plot of soil moisture and irrigation amounts retrieved by PrISM for the Foradada field in 2020. Same description as in Fig. 8.

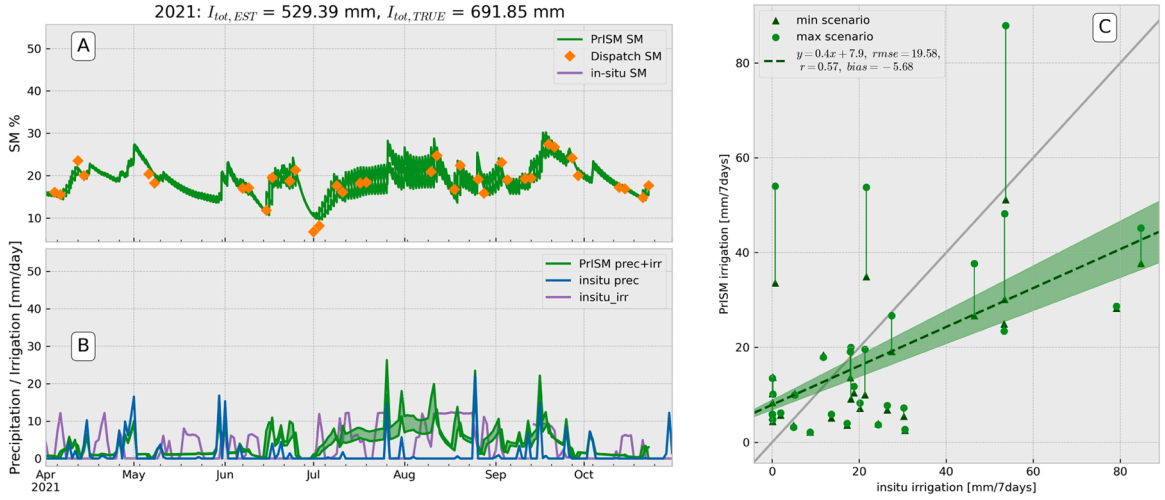

Fig. B.4. time series and scatter plot of soil moisture and irrigation amounts retrieved by PrISM for the Foradada field in 2021. Same description as in Fig. 8.

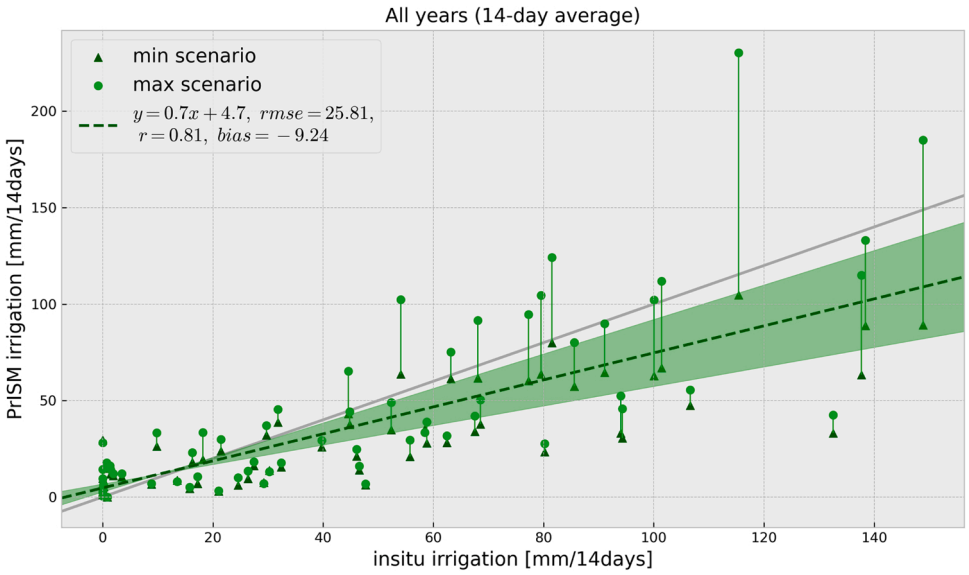

Fig. B.5. Final scatter plot field level (aggregated at biweekly level) for all the years.

precipitation was retrieved from a dense network of in situ meteo stations, ensuring a high fidelity of the product. Errors in precipitation timings and amounts will directly affect the irrigation retrieval, since irrigation is retrieved by subtraction to the initial precipitation profile, similar to other approaches for irrigation estimation and timing (Dari et al., 2020; Abolafia-Rosenzweig et al., 2019; Zappa et al., 2022; Le Page et al., 2023) and precipitation is always assumed as exempt from errors. Remote sensing precipitation products may not always be available at high temporal or spatial resolution, causing a possible degradation of the results. In particular, when using a precipitation dataset with a lower temporal resolution in PrISM, it is expected that the maximum and minimum irrigation scenarios will tend to be closer to each other and the quality of the amounts of irrigation will decrease, up to the edge case where precipitation and soil moisture used have the same temporal resolution, and the two scenarios represent the same amount of irrigation.

As demonstrated by Jalilvand et al. (2019), implementing a bias correction post-processing step in the methodology improves the retrieval of irrigation amounts. This approach removes the bias by subtracting the false irrigation amounts detected in the adjacent non-irrigated pixel from the actual irrigated pixel. This post-processing step could be a straightforward implementation in PrISM, as adjacent non-irrigated pixels are already identified and used for calibration. With this approach, false detection of irrigation events (mostly linked to missing precipitation events in the initial datasets, which are then classified as irrigation) is expected to be mitigated.

New *SM* products are expected to be available in the near future, such as the SMOS-HR mission (Rodríguez-Fernández et al., 2019) and ROSE-L mission (Pierdicca et al., 2019), which could provide access to higher spatial resolution *SM* observations and allow for combination of multiple *SM* products from different sources, which in turn will increase temporal and spatial availability of this variable. The advent of these new products will allow for a more precise estimation of irrigation amounts at the field level.

Declaration of Competing Interest

The authors declare that they have no known competing financial interests or personal relationships that could have appeared to influence the work reported in this paper.

Data availability

Data will be made available on request.

Acknowledgements

The first author received the grant DIN2019–010652 from the Spanish Education Ministry (MICINN) and DI-2020-093 from the Catalan Agency of Research (AGAUR). We are grateful for the financial support given by the ACCWA project, funded by the European Commission Horizon 2020 Program for Research and Innovation, in the context of the Marie Skłodowska-Curie Research and Innovation Staff Exchange (RISE) action under the grant agreement No. 823965, and by the PRIMA ALTOS project (No. PCI2019–103649) of the Ministry of Science, Innovation and Universities of the Spanish government. The PRIMA IDEWA project is also acknowledged.

Appendix A. Additional results from the synthetic study

Additional tests were performed for the case where observed *SM* was retrieved from a pixel covering an area that is only partially irrigated (simulated using different fractions of irrigated area). Synthetic *SM* observations were built using three different fractions of the irrigated area: 100%, 80%, and 40%. Additionally, different temporal frequencies and observation noises were evaluated, as in Fig. 5. The tests were performed using the two scenarios of PrISM presented in this study: unconstrained and constrained with daily irrigation frequencies. Fig. Appendix A.1 shows the results in terms of total cumulative error and Pearson's correlation r.ăResults indicate how decreasing irrigation percentages in the pixel leads to a sharp underestimation of the total amount of irrigation and precipitation, and it also leads to worse performances in terms of *r* for the unconstrained scenario. The constrained scenario shows better performances in terms of *r* for all the cases, but the total amount of irrigation is still underestimated. This is because the irrigation signal is mixed with the signal from dryland in the *SM* observation and the model is not able to account for that. A future postprocessing approach could account for different fractions of irrigated area for each pixel (using a map of irrigated fields) and correct the underestimation effect by simply dividing the retrieved irrigation amounts by the fraction of irrigated area.

B. Additional Results from the Foradada field

PrISM for irrigation amount retrieval was applied to the Foradada field from 2017 and 2021. Fig. Appendix B.1, B.2, B.3 to Appendix B.4 show the results in terms of time series and scatter plots of the retrieved irrigation amounts and *SM* observations as it was presented for the year 2017 in Fig. 8. Finally, Fig. 9 shows the comparison for all the years between in-situ and estimated irrigation amounts, at a bi-weekly scale Fig. B.5.

References

Abolafia-Rosenzweig, R., Livneh, B., Small, E., Kumar, S., 2019. Soil moisture data assimilation to estimate irrigation water use. J. Adv. Model. Earth Syst. 11, 3670–3690. https://doi.org/10.1029/2019MS001797.

Alexandratos, N., Bruinsma, J., 2012.World Agriculture towards 2030/2050: The 2012 Revision. ESA Working paper No. 12–03, Rome, FAO.

Balasubramanya, S., Stifel, D., 2020. Viewpoint: water, agriculture & poverty in an era of climate change: why do we know so little? Food Policy 93, 101905. https://doi.org/10.1016/j.foodpol.2020.101905.

Brocca, L., Ciabatta, L., Massari, C., Moramarco, T., Hahn, S., Hasenauer, S., Kidd, R., Dorigo, W., Wagner, W., Levizzani, V., 2014. Soil as a natural rain gauge: estimating global rainfall from satellite soil moisture data. J. Geophys. Res.: Atmospheres 119, 5128–5141. https://doi.org/10.1002/2014JD021489.

Brocca, L., Pellarin, T., Crow, W.T., Ciabatta, L., Massari, C., Ryu, D., Su, C.H., Rüdiger, C., Kerr, Y., 2016. Rainfall estimation by inverting SMOS soil moisture estimates: a comparison of different methods over Australia. J. Geophys. Res.: Atmospheres 121, 12,062–12,079. https://doi.org/10.1002/2016JD025382.

Brocca, L., Tarpanelli, A., Filippucci, P., Dorigo, W., Zaussinger, F., Gruber, A., Fernández-Prieto, D., 2018. How much water is used for irrigation? A new approach exploiting coarse resolution satellite soil moisture products. Int. J. Appl. Earth Obs. Geoinf. 73, 752–766. https://doi.org/10.1016/j.jag.2018.08.023.

Brombacher, J., Silva, I.R.d.O., Degen, J., Pelgrum, H., 2022. A novel evapotranspiration based irrigation quantification method using the hydrological similar pixels algorithm. Agric. Water Manag. 267, 107602 https://doi.org/10.1016/j.agwat.2022.107602.

Coates, D., Connor, R., Leclerc, L., Rast, W., Schumann, K., Webber, M., 2012. CHAPTER 2 Water demand: What drives consumption? The United Nations World Water Development Report 4: Managing Water Report under Uncertainty and Risk, 1 ed..,. UNESCO,, Paris.

Crow, W.T., Loon, E.V., 2006. Impact of incorrect model error assumptions on the sequential assimilation of remotely sensed surface soil moisture. J. Hydrometeorol. 7, 421–432. https://doi.org/10.1175/JHM499.1.

Dari, J., Brocca, L., Quintana-Seguí, P., Escorihuela, M.J., Stefan, V., Morbidelli, R., 2020. Exploiting high-resolution remote sensing soil moisture to estimate irrigation water amounts over a Mediterranean Region. Remote Sens. 12, 2593. https://doi.org/10.3390/rs12162593.

Dari, J., Quintana-Seguí, P., Morbidelli, R., Saltalippi, C., Flammini, A., Giugliarelli, E., Escorihuela, M.J., Stefan, V., Brocca, L., 2022. Irrigation estimates from space: implementation of different approaches to model the evapotranspiration contribution within a soil-moisture-based inversion algorithm. Agric. Water Manag. 265, 107537 https://doi.org/10.1016/j.agwat.2022.107537.

Dari, J., Brocca, L., Modanesi, S., Massari, C., Tarpanelli, A., Barbetta, S., Quast, R., Vreugdenhil, M., Freeman, V., Barella-Ortiz, A., Quintana-Seguí, P., Bretreger, D., Volden, E., 2023. Regional data sets of high-resolution (1 and 6 km) irrigation estimates from space. Earth Syst. Sci. Data 15, 1555–1575. https://doi.org/10.5194/essd-15-1555-2023.

Descroix, L., Nouvelot, J.F., Vauclin, M., 2002. Evaluation of an antecedent precipitation index to model runoff yield in the western Sierra Madre (North-west Mexico). J. Hydrol. 263, 114–130. https://doi.org/10.1016/S0022-1694(02)00047-1.

Droogers, P., Immerzeel, W.W., Lorite, I.J., 2010. Estimating actual irrigation application by remotely sensed evapotranspiration observations. Agric. Water Manag. 97, 1351–1359. https://doi.org/10.1016/j.agwat.2010.03.017.

Entekhabi, D., Njoku, E.G., O'Neill, P.E., Kellogg, K.H., Crow, W.T., Edelstein, W.N., Entin, J.K., Goodman, S.D., Jackson, T.J., Johnson, J., Kimball, J., Piepmeier, J.R., Koster, R.D., Martin, N., McDonald, K.C., Moghaddam, M., Moran, S., Reichle, R., Shi, J.C., Spencer, M.W., Thurman, S.W., Tsang, L., Van Zyl, J., 2010.The Soil Moisture Active Passive (SMAP) Mission.Proceedings of the IEEE 98, 704–716.10.1109/JPROC.2010.2043918.

Escorihuela, M.J., Quintana-Seguí, P., 2016. Comparison of remote sensing and simulated soil moisture datasets in Mediterranean landscapes. Remote Sens. Environ. 180, 99–114. https://doi.org/10.1016/j.rse.2016.02.046.

Ferguson, I.M., Maxwell, R.M., 2012. Human impacts on terrestrial hydrology: climate change versus pumping and irrigation. Environ. Res. Lett. 7, 044022 https://doi.org/10.1088/1748-9326/7/4/044022.

Filippucci, P., Tarpanelli, A., Massari, C., Serafini, A., Strati, V., Alberi, M., Raptis, K.G. C., Mantovani, F., Brocca, L., 2020. Soil moisture as a potential variable for tracking and quantifying irrigation: a case study with proximal gamma-ray spectroscopy data. Adv. Water Resour. 136, 103502 https://doi.org/10.1016/j.advwatres.2019.103502.

Fischer, G., Tubiello, F.N., van Velthuizen, H., Wiberg, D.A., 2007. Climate change impacts on irrigation water requirements: effects of mitigation, 1990–2080. Technol. Forecast. Soc. Change 74, 1083–1107. https://doi.org/10.1016/j.techfore.2006.05.021.

Foley, J.A., Ramankutty, N., Brauman, K.A., Cassidy, E.S., Gerber, J.S., Johnston, M., Mueller, N.D., O'Connell, C., Ray, D.K., West, P.C., Balzer, C., Bennett, E.M., Carpenter, S.R., Hill, J., Monfreda, C., Polasky, S., Rockström, J., Sheehan, J., Siebert, S., Tilman, D., Zaks, D.P.M., 2011. Solutions for a cultivated planet. Nature 478, 337–342. https://doi.org/10.1038/nature10452.

Folhes, M.T., Rennó, C.D., Soares, J.V., 2009. Remote sensing for irrigation water management in the semi-arid Northeast of Brazil. Agric. Water Manag. 96, 1398–1408. https://doi.org/10.1016/j.agwat.2009.04.021.

Fontanet, M., Fernàndez-Garcia, D., Ferrer, F., 2018. The value of satellite remote sensing soil moisture data and the DISPATCH algorithm in irrigation fields. Hydrol. Earth Syst. Sci. 22, 5889–5900. https://doi.org/10.5194/hess-22-5889-2018.

Foster, T., Mieno, T., Brozović, N., 2020. Satellite-based monitoring of irrigation water use: assessing measurement errors and their implications for agricultural water management policy. Water Resour. Res. 56, e2020WR028378 https://doi.org/10.1029/2020WR028378.

Gleick, P.H., 2014. The Worldas Water (Ed.). Island Press/Center for Resource Economics,, Washington, DC. https://doi.org/10.5822/978-1-61091-483-3.

Haddeland, I., Heinke, J., Biemans, H., Eisner, S., Flörke, M., Hanasaki, N., Konzmann, M., Ludwig, F., Masaki, Y., Schewe, J., Stacke, T., Tessler, Z.D., Wada, Y., Wisser, D., 2014. Global water resources affected by human interventions and climate change. Proc. Natl. Acad. Sci. 111, 3251–3256. https://doi.org/10.1073/pnas.1222475110.

Hamze, M., Cheviron, B., Baghdadi, N., Lo, M., Courault, D., Zribi, M., 2023. Detection of irrigation dates and amounts on maize plots from the integration of Sentinel-2 derived Leaf Area Index values in the Optirrig crop model. Agric. Water Manag. 283, 108315 https://doi.org/10.1016/j.agwat.2023.108315.

Harding, K.J., Snyder, P.K., 2012. Modeling the atmospheric response to irrigation in the great plains. Part I: general impacts on precipitation and the energy budget. J. Hydrometeorol. 13, 1667–1686. https://doi.org/10.1175/JHM-D-11-098.1.

Hejazi, M., Edmonds, J., Clarke, L., Kyle, P., Davies, E., Chaturvedi, V., Wise, M., Patel, P., Eom, J., Calvin, K., Moss, R., Kim, S., 2014. Long-term global water projections using six socioeconomic scenarios in an integrated assessment modeling framework. Technol. Forecast. Soc. Change 81, 205–226. https://doi.org/10.1016/j.techfore.2013.05.006.

Jalilvand, E., Tajrishy, M., GhaziZadehHashemi, S.A., Brocca, L., 2019. Quantification of irrigation water using remote sensing of soil moisture in a semi-arid region. Remote Sens. Environ. 231, 111226 https://doi.org/10.1016/j.rse.2019.111226.

Jalilvand, E., Abolafia-Rosenzweig, R., Tajrishy, M., Kumar, S.V., Mohammadi, M.R., Das, N.N., 2023. Is it possible to quantify irrigation water-use by assimilating a high-resolution satellite soil moisture product? Water Resour. Res. 59, e2022WR033342 https://doi.org/10.1029/2022WR033342.

Koch, J., Zhang, W., Martinsen, G., He, X., Stisen, S., 2020 (Estimating Net Irrigation Across the North China Plain Through Dual Modeling of Evapotranspiration.). Water Resour. Res. 56, e2020WR027413. https://doi.org/10.1029/2020WR027413.

Kragh, S.J., Fensholt, R., Stisen, S., Koch, J., 2023. The precision of satellite-based net irrigation quantification in the Indus and Ganges basins. Hydrol. Earth Syst. Sci. 27, 2463–2478. https://doi.org/10.5194/hess-27-2463-2023.

Kumar, S.V., Peters-Lidard, C.D., Santanello, J.A., Reichle, R.H., Draper, C.S., Koster, R. D., Nearing, G., Jasinski, M.F., 2015. Evaluating the utility of satellite soil moisture retrievals over irrigated areas and the ability of land data assimilation methods to correct for unmodeled processes. Hydrol. Earth Syst. Sci. 19, 4463–4478. https://doi.org/10.5194/hess-19-4463-2015.

Lawston, P.M., Santanello Jr, J.A., Kumar, S.V., 2017. Irrigation signals detected from SMAP soil moisture retrievals. Geophys. Res. Lett. 44, 11,860–11,867. https://doi.org/10.1002/2017GL075733.

Le Page, M., Nguyen, T., Zribi, M., Boone, A., Dari, J., Modanesi, S., Zappa, L., Ouaadi, N., Jarlan, L., 2023. Irrigation timing retrieval at the plot scale using surface soil moisture derived from sentinel time series in Europe. Remote Sens. 15, 1449. https://doi.org/10.3390/rs15051449.

Maneewongvatana, S., Mount, D.M., 1999.Analysis of approximate nearest neighbor searching with clustered point sets. arXiv:cs/9901013.

Maselli, F., Battista, P., Chiesi, M., Rapi, B., Angeli, L., Fibbi, L., Magno, R., Gozzini, B., 2020. Use of Sentinel-2 MSI data to monitor crop irrigation in Mediterranean areas. Int. J. Appl. Earth Obs. Geoinf. 93, 102216 https://doi.org/10.1016/j.jag.2020.102216.

Massari, C., Modanesi, S., Dari, J., Gruber, A., De Lannoy, G.J.M., Girotto, M., Quintana-Seguí, P., LePage, M., Jarlan, L., Zribi, M., Ouaadi, N., Vreugdenhil, M., Zappa, L., Dorigo, W., Wagner, W., Brombacher, J., Pelgrum, H., Jaquot, P., Freeman, V., Volden, E., Fernandez Prieto, D., Tarpanelli, A., Barbetta, S., Brocca, L., 2021. A review of irrigation information retrievals from space and their utility for users. Remote Sens. 13, 4112. https://doi.org/10.3390/rs13204112.

McDermid, S., Nocco, M., Lawston-Parker, P., Keune, J., Pokhrel, Y., Jain, M., Jägermeyr, J., Brocca, L., Massari, C., Jones, A.D., Vahmani, P., Thiery, W., Yao, Y., Bell, A., Chen, L., Dorigo, W., Hanasaki, N., Jasechko, S., Lo, M.H., Mahmood, R., Mishra, V., Mueller, N.D., Niyogi, D., Rabin, S.S., Sloat, L., Wada, Y., Zappa, L., Chen, F., Cook, B.I., Kim, H., Lombardozzi, D., Polcher, J., Ryu, D., Santanello, J., Satoh, Y., Seneviratne, S., Singh, D., Yokohata, T., 2023. Irrigation in the Earth system. Nat. Rev. Earth Environ. 4, 435–453. https://doi.org/10.1038/s43017-023-00438-5.

Merlin, O., Rudiger, C., AlBitar, A., Richaume, P., Walker, J.P., Kerr, Y.H., 2012. Disaggregation of SMOS Soil Moisture in Southeastern Australia. IEEE Trans. Geosci. Remote Sens. 50, 1556–1571. https://doi.org/10.1109/TGRS.2011.2175000.

Merlin, O., Escorihuela, M.J., Mayoral, M.A., Hagolle, O., AlBitar, A., Kerr, Y., 2013. Self-calibrated evaporation-based disaggregation of SMOS soil moisture: an evaluation

study at 3km and 100m resolution in Catalunya, Spain. Remote Sens. Environ. 130, 25–38. https://doi.org/10.1016/j.rse.2012.11.008.
Modanesi, S., Massari, C., Bechtold, M., Lievens, H., Tarpanelli, A., Brocca, L., Zappa, L., De Lannoy, G.J.M., 2022. Challenges and benefits of quantifying irrigation through the assimilation of Sentinel-1 backscatter observations into Noah-MP. Hydrol. Earth Syst. Sci. 26, 4685–4706. https://doi.org/10.5194/hess-26-4685-2022.
Molero, B., Merlin, O., Malbéteau, Y., AlBitar, A., Cabot, F., Stefan, V., Kerr, Y., Bacon, S., Cosh, M., Bindlish, R., Jackson, T., 2016. SMOS disaggregated soil moisture product at 1 km resolution: processor overview and first validation results. Remote Sens. Environ. 180, 361–376. https://doi.org/10.1016/j.rse.2016.02.045.
Moradkhani, H., Hsu, K.L., Gupta, H., Sorooshian, S., 2005. Uncertainty assessment of hydrologic model states and parameters: sequential data assimilation using the particle filter. Water Resour. Res. 41 https://doi.org/10.1029/2004WR003604.
N.J. Gordon D.J. Salmond A.F.M. Smith Novel approach to nonlinear/non-Gaussian Bayesian state estimation IEE Proc. F. (Radar Signal Process.) 140 1993 107 113 doi: 10.1049/ip-f-2.1993.0015.
Nie, W., Kumar, S.V., Bindlish, R., Liu, P.W., Wang, S., 2022. Remote sensing-based vegetation and soil moisture constraints reduce irrigation estimation uncertainty. Environ. Res. Lett. 17, 084010 https://doi.org/10.1088/1748-9326/ac7ed8.
Niu, G.Y., Yang, Z.L., Mitchell, K.E., Chen, F., Ek, M.B., Barlage, M., Kumar, A., Manning, K., Niyogi, D., Rosero, E., Tewari, M., Xia, Y., 2011. The community Noah land surface model with multiparameterization options (Noah-MP): 1. Model description and evaluation with local-scale measurements. J. Geophys. Res.: Atmospheres 116. https://doi.org/10.1029/2010JD015139.
OECD, 2015. Drying Wells, Rising Stakes; Towards Sustainable Agricultural Groundwater Use. OECD studies on water ed. OECD Publishing,, Paris.
Ojha, N., Merlin, O., Suere, C., Escorihuela, M.J., 2021. Extending the Spatio-Temporal Applicability of DISPATCH soil moisture downscaling algorithm: a study case using SMAP, MODIS and Sentinel-3 Data. Front. Environ. Sci. 9.
Olivera-Guerra, L., Merlin, O., Er-Raki, S., Khabba, S., Escorihuela, M.J., 2018. Estimating the water budget components of irrigated crops: combining the FAO-56 dual crop coefficient with surface temperature and vegetation index data. Agric. Water Manag. 208, 120–131. https://doi.org/10.1016/j.agwat.2018.06.014.
Olivera-Guerra, L.E., Laluet, P., Altés, V., Ollivier, C., Pageot, Y., Paolini, G., Chavanon, E., Rivalland, V., Boulet, G., Villar, J.M., Merlin, O., 2023. Modeling actual water use under different irrigation regimes at district scale: application to the FAO-56 dual crop coefficient method. Agric. Water Manag. 278, 108119 https://doi.org/10.1016/j.agwat.2022.108119.
Ouaadi, N., Jarlan, L., Khabba, S., Ezzahar, J., LePage, M., Merlin, O., 2021. Irrigation amounts and timing retrieval through data assimilation of surface soil moisture into the FAO-56 approach in the South Mediterranean Region. Remote Sens. 13, 2667. https://doi.org/10.3390/rs13142667.
Ozdogan, M., Yang, Y., Allez, G., Cervantes, C., 2010. Remote sensing of irrigated agriculture: opportunities and challenges. Remote Sens. 2, 2274–2304. https://doi.org/10.3390/rs2092274.
Pan, F., Peters-Lidard, C.D., Sale, M.J., 2003. An analytical method for predicting surface soil moisture from rainfall observations. Water Resour. Res. 39. https://doi.org/10.1029/2003WR002142.
Paolini, G., Escorihuela, M.J., Merlin, O., Sans, M.P., Bellvert, J., 2022. Classification of different irrigation systems at field scale using time-series of remote sensing data. IEEE J. Sel. Top. Appl. Earth Obs. Remote Sens. 15, 10055–10072. https://doi.org/10.1109/JSTARS.2022.3222884.
Pellarin, T., Louvet, S., Gruhier, C., Quantin, G., Legout, C., 2013. A simple and effective method for correcting soil moisture and precipitation estimates using AMSR-E measurements. Remote Sens. Environ. 136, 28–36. https://doi.org/10.1016/j.rse.2013.04.011.
Pellarin, T., Román-Cascón, C., Baron, C., Bindlish, R., Brocca, L., Camberlin, P., Fernández-Prieto, D., Kerr, Y.H., Massari, C., Panthou, G., Perrimond, B., Philippon, N., Quantin, G., 2020. The Precipitation Inferred from Soil Moisture (PrISM) near real-time rainfall product: evaluation and comparison. Remote Sens. 12, 481. https://doi.org/10.3390/rs12030481.
Peng, J., Albergel, C., Balenzano, A., Brocca, L., Cartus, O., Cosh, M.H., Crow, W.T., Dabrowska-Zielinska, K., Dadson, S., Davidson, M.W.J., de Rosnay, P., Dorigo, W., Gruber, A., Hagemann, S., Hirschi, M., Kerr, Y.H., Lovergine, F., Mahecha, M.D., Marzahn, P., Mattia, F., Musial, J.P., Preuschmann, S., Reichle, R.H., Satalino, G., Silgram, M., van Bodegom, P.M., Verhoest, N.E.C., Wagner, W., Walker, J.P., Wegmüller, U., Loew, A., 2021. A roadmap for high-resolution satellite soil moisture applications – confronting product characteristics with user requirements. Remote Sens. Environ. 252, 112162 https://doi.org/10.1016/j.rse.2020.112162.
Pierdicca, N., Davidson, M., Chini, M., Dierking, W., Djavidnia, S., Haarpaintner, J., Hajduch, G., Laurin, G.V., Lavalle, M., López-Martínez, C., Nagler, T., Su, B., 2019. The Copernicus L-band SAR mission ROSE-L (Radar Observing System for Europe) (Conference Presentation). Active and Passive Microwave Remote Sensing for Environmental Monitoring III. SPIE,, p. 111540E. https://doi.org/10.1117/12.2534743.
Riediger, J., Breckling, B., Nuske, R.S., Schröder, W., 2014. Will climate change increase irrigation requirements in agriculture of Central Europe? A simulation study for Northern Germany. Environ. Sci. Eur. 26, 18. https://doi.org/10.1186/s12302-014-0018-1.
Rodríguez-Fernández, N.J., Anterrieu, E., Rougé, B., Boutin, J., Picard, G., Pellarin, T., Escorihuela, M.J., AlBitar, A., Richaume, P., Mialon, A., Merlin, O., Suere, C., Cabot, F., Khazaal, A., Costeraste, J., Palacin, B., Rodriguez-Suquet, R., Tournier, T., Decoopman, T., Colom, M., Morel, J.M., Kerr, Y.H., 2019.SMOS-HR: A High Resolution L-Band Passive Radiometer for Earth Science and Applications, in: IGARSS 2019 - 2019 IEEE International Geoscience and Remote Sensing Symposium, 8392–8395.10.1109/IGARSS.2019.8897815.
Román-Cascón, C., Pellarin, T., Gibon, F., Brocca, L., Cosme, E., Crow, W., Fernández-Prieto, D., Kerr, Y.H., Massari, C., 2017. Correcting satellite-based precipitation products through SMOS soil moisture data assimilation in two land-surface models of different complexity: aaa and SURFEX. Remote Sens. Environ. 200, 295–310. https://doi.org/10.1016/j.rse.2017.08.022.
Sacks, W.J., Cook, B.I., Buenning, N., Levis, S., Helkowski, J.H., 2009. Effects of global irrigation on the near-surface climate. Clim. Dyn. 33, 159–175. https://doi.org/10.1007/s00382-008-0445-z.
Sittner, W.T., Schauss, C.E., Monro, J.C., 1969. Continuous hydrograph synthesis with an API-type hydrologic model. Water Resour. Res. 5, 1007–1022. https://doi.org/10.1029/WR005i005p01007.
de Vrese, P., Hagemann, S., Claussen, M., 2016. Asian irrigation, African rain: Remote impacts of irrigation. Geophys. Res. Lett. 43, 3737–3745. https://doi.org/10.1002/2016GL068146.
Wada, Y., van Beek, L.P.H., Bierkens, M.F.P., 2011. Modelling global water stress of the recent past: on the relative importance of trends in water demand and climate variability. Hydrol. Earth Syst. Sci. 15, 3785–3808. https://doi.org/10.5194/hess-15-3785-2011.
Wada, Y., Wisser, D., Eisner, S., Flörke, M., Gerten, D., Haddeland, I., Hanasaki, N., Masaki, Y., Portmann, F.T., Stacke, T., Tessler, Z., Schewe, J., 2013. Multimodel projections and uncertainties of irrigation water demand under climate change. Geophys. Res. Lett. 40, 4626–4632. https://doi.org/10.1002/grl.50686.
Yan, H., DeChant, C.M., Moradkhani, H., 2015. Improving soil moisture profile prediction with the particle filter-markov Chain Monte Carlo Method. IEEE Trans. Geosci. Remote Sens. 53, 6134–6147. https://doi.org/10.1109/TGRS.2015.2432067.
Yao, Y., Vanderkelen, I., Lombardozzi, D., Swenson, S., Lawrence, D., Jägermeyr, J., Grant, L., Thiery, W., 2022. Implementation and evaluation of irrigation techniques in the community land model. J. Adv. Model. Earth Syst. 14, e2022MS003074 https://doi.org/10.1029/2022MS003074.
Zappa, L., Schlaffer, S., Bauer-Marschallinger, B., Nendel, C., Zimmerman, B., Dorigo, W., 2021. Detection and quantification of irrigation water amounts at 500 m using Sentinel-1 surface soil moisture. Remote Sens. 13, 1727. https://doi.org/10.3390/rs13091727.
Zappa, L., Schlaffer, S., Brocca, L., Vreugdenhil, M., Nendel, C., Dorigo, W., 2022. How accurately can we retrieve irrigation timing and water amounts from (satellite) soil moisture? Int. J. Appl. Earth Obs. Geoinf. 113, 102979 https://doi.org/10.1016/j.jag.2022.102979.
Zaussinger, F., Dorigo, W., Gruber, A., Tarpanelli, A., Filippucci, P., Brocca, L., 2019. Estimating irrigation water use over the contiguous United States by combining satellite and reanalysis soil moisture data. Hydrol. Earth Syst. Sci. 23, 897–923. https://doi.org/10.5194/hess-23-897-2019.
Zhang, C., Long, D., 2021. Estimating spatially explicit irrigation water use based on remotely sensed evapotranspiration and modeled root zone soil moisture. Water Resour. Res. 57, e2021WR031382 https://doi.org/10.1029/2021WR031382.
Zhu, B., Huang, M., Cheng, Y., Xie, X., Liu, Y., Zhang, X., Bisht, G., Chen, X., Missik, J., Liu, H., 2020. Effects of irrigation on water, carbon, and nitrogen budgets in a semiarid watershed in the pacific northwest: a modeling study. J. Adv. Model. Earth Syst. 12, e2019MS001953 https://doi.org/10.1029/2019MS001953.